March 2015

# FLOW DISTRIBUTION CONTROL IN MESO SCALE VIA ELECTROHYDRODYNAMIC CONDUCTION PUMPING

Brandon Charles Shaw
*Worcester Polytechnic Institute*

Cheng Jiang
*Worcester Polytechnic Institute*

Kliment Sashev Minchev
*Worcester Polytechnic Institute*

Follow this and additional works at: https://digitalcommons.wpi.edu/mqp-all

# FLOW GENERATION AND DISTRIBUTION CONTROL IN MESO SCALE VIA ELECTROHYDRODYNAMIC CONDUCTION PUMPING

A Major Qualifying Project
Submitted to the Faculty of
Worcester Polytechnic Institute
in partial fulfillment of the requirements for the
Degree in Bachelor of Science
in
Mechanical Engineering
By

_____

Cheng Jiang

_____

Kliment S. Minchev

_____

Brandon C. Shaw

Date: 3/25/2015

Project Advisor:

_____

Dr. Jamal Seyed-Yagoobi

## Abstract

Electrohydrodynamic (EHD) conduction pumping technology offers a unique way to control flow distribution in multi-scale environments. In EHD conduction, the interaction between an applied electrical field and dissociated electrolyte species in a dielectric fluid generates a net body force within the fluid, resulting in a net flow in the desired direction. EHD conduction pumps have remarkable potential due to their lack of moving parts, simple designs, low power consumption, and ability to operate in microgravity. The performance of these pumps increases at small scales and they have been previously proven effective for heat transfer enhancement, with possible applications in electronics cooling and more, both terrestrially and in space. Flow distribution control using EHD conduction pumps was previously examined in a macro-scale configuration. This experimental study examined flow distribution control among three 1 mm-diameter parallel tubes utilizing EHD conduction pumps in meso-scale. The resulting data supports the application of EHD pumping to flow distribution control by exemplifying the system performances at various overall induced flow rates. The EHD pumps were able to successfully correct maldistributed flow in other branch lines as well as being able to introduce maldistribution in branch lines where even flow was initialized, including depriving other channels of flow. The micro-scale EHD pumps were operated between 0V and 1500V, with supply flow rates between 3mL/min and 25mL/min.

**Acknowledgements**

## Table of Contents

## Table of Figures

**Table of Tables**

**Chapter 1: Introduction**

**1.1 Overview**

Electrohydrodynamics (EHD) is the field of study associated with the motion of charged fluids under the influence of electric fields. The most valuable application of EHD is pumping, the ability to generate flow in an electrically charged fluid. There are three major types of EHD pumping: conduction, induction, and ion-drag, the difference between which is the technique used to produce charges in the fluid.

The goal of this Major Qualifying Project was to study the capability of EHD conduction pumping to control flow distribution in parallel meso-scale branches using micro-scale pumps. A loop was assembled in order to show the successful generation of flow and pressure. Using a complex system of sensors and data acquisition modules, it was established that the flow could be redistributed and manipulated by varying the electric field imposed on the EHD pumps. A set of experiments provided proof that micro-scale EHD conduction pumps are able to control the flow in parallel meso-scale branches. The conclusions from this study could be directly applied to solve a wide range of fundamental problems in the engineering industry. Applications in thermal system flow control, microelectronic cooling and microgravity orbital heat transfer enhancement are a few of the examples where EHD micro-scale conduction pumping could potentially revolutionize performance and maximize efficiency.

There are certain known advantages of EHD conduction pumps over standard mechanical pumps. The pumps are typically lightweight, have a simplistic design with no moving parts, and need minimal to no maintenance. They have the ability to operate in microgravity conditions due to their operational independence from gravity [7] and their low power requirement. EHD

conduction pumps provide intelligent control by varying the electric field applied to its

electrodes and are applicable to single and two-phase flow [1].

This study is a continuation of the research conducted by Feng, Patel, and Seyed-

Yagoobi. The importance of the results is related to the potential application of EHD conduction

pumping in micro-scale, which would eventually lead to efficient flow distribution control and

heat transfer enhancement in cutting-edge technology.

## 1.2 Theoretical Basis

### 1.2.1 Mathematical Basis

The study of Electrohydrodynamics (EHD) investigates the flow of electrically charged

fluids by examining the interactions between electric fields and the forces related to the resulting

fluid flow. Under EHD pumping, the flow of the fluid is triggered by charge transport. Each of

the three major EHD pumping mechanisms uses a distinct method of injecting charges into the

working fluid. As a result of the presence of an electric field, the charges displace and carry the

fluid, which summarizes the EHD pumping effect. Even though EHD pumping is an innovative

method of generating fluid flow, fluid electrokinetic properties were first theoretically described

over a century ago. After a variety of experiments were conducted throughout the 20th century to

test and establish its capabilities, the EHD pumping phenomenon can be defined by an electric

field resulting in fluid pumping and flow control.

The Coulomb force caused by the high voltage, along with the Dielectrophoretic (DEP)

force and Electrostriction force are the three most dominant EHD forces under consideration.

The Coulomb force is based on Coulomb's Law, a well-known phenomenon in

electromagnetism. Coulomb's Law describes a directly proportional relationship between electric field (E) and body force on a point charge (F). The Dielectrophoretic (DEP) force occurs when there is a non-uniform electric field present, which evokes dielectrophoretic behavior in all fluid particles regardless of their charge. This dielectrophoretic behavior is described by the polarization of the fluid particles causing the dipoles to experience the DEP force along the lines of the electric field. The Electrostriction force is represented by the ion displacement within the structure of the fluid particles, which describes changes to the shape of each particle. Even though it is somewhat insignificant to the overall body force, the Electrostriction force contributes to the fluid flow on an infinitesimal level. As a result of both mathematical analysis and testing, in single-phase dielectric liquid flow, the DEP and Electrostriction forces could be neglected when estimating the total electric body force due to their insignificant magnitudes and effects [2].

In order to understand the EHD phenomenon in depth, research has uncovered a thorough mathematical study of the forces acting of the fluid particles. Knowing that there is an overall flow rate generated by an EHD pump, it can be concluded that there is a net force applied to the fluid. Eliminating all other non-EHD forces that could be imposed on the fluid, the net body force experienced by the fluid is a sum of the Coulomb force caused by the applied electric field, the Dielectrophoretic (DEP) force caused by the non-uniformity in the electric field, and the Electrostriction force caused by the ion displacement within the structure of the fluid particles. This statement is summarized by the following equation:

$$\overrightarrow{F_E} = q\vec{E} - \frac{1}{2}E^2\nabla\epsilon + \nabla[\rho\frac{E^2}{2}\left(\frac{\partial\epsilon}{\partial\rho}\right)_T]$$

According to Coulomb's law, $E = \frac{F}{q} \rightarrow F = qE$, where E is the strength of the applied electric field, F is the Coulomb force and q is the charge density of the fluid particle. The DEP force is described by the strength of the electric field and a gradient of ε, the fluid permittivity. The permittivity of an electromagnetic medium is a constant property describing the resistance to an applied electric field. The Electrostriction force is described by the fluid density, magnitude of the applied electric field, and a gradient in permittivity [2].

In a single-phase liquid with no change in temperature however, there would be no gradient in permittivity or infinitesimal change in density. Thus, the net force experienced by the fluid would only be a result of the Coulomb force. Therefore, assuming the EHD pump system uses an isothermal single-phase liquid, the equation simplifies to:

$$\vec{F_E} = q\vec{E}$$

### 1.2.2 Types of EHD Pumping Mechanisms

EHD pumping is based on the presence of an electric field and its interaction with a working fluid. However, EHD pumping is divided into three distinct types based on the technique used to introduce charges to the fluid.

EHD conduction pumping is a result of applying a high voltage electric field across an organized set of electrodes on to a dielectric fluid to achieve flow [1]. On a molecular level, when subjected to an electric field, the working fluid experiences dissociation and recombination of ions. According to the basic property of chemical equilibrium for reversible reactions, the dielectric impurities in the fluid constantly separate into charged ions and recombine back into neutrally charged molecules at an equal rate [1]. These equal rates result in overall charge equilibrium.

Under high-voltage electric fields, however (e.g. greater than $10^3$ V/cm) [3], the rate of dissociation increases, whereas recombination remains relatively constant. Thus, above this critical voltage threshold, the rate of the field-enhanced dissociation is greater than the rate of recombination, which results in non-equilibrium conditions. As a result, a uniformly charged layer of ions, referred to as the heterocharge layer [1], forms along each of the electrodes. These heterocharge layers attract to the oppositely charged electrodes (e.g. positively charged layers attract towards the ground electrodes and negatively charged layers attract towards the positively charged high voltage electrodes). Since the Coulomb forces would usually balance each other if the electrodes were identical in size, the high voltage electrodes are specifically designed to form drastically larger heterocharge layers and thus create non-equilibrium forces.

**EHD Ion-Drag Pumping**

The oldest known EHD flow generation phenomenon is EHD Ion-Drag pumping, which includes a charge-injecting emitting source electrode and a collecting electrode. The emitting source provides charge injection through a corona discharge. The corona discharge forms in the presence of a very high voltage source imposing a localized electric field, which ionizes the surrounding fluid. As a result, charges are periodically pumped into the fluid, which then shift forward along the lines of the electric field formed between the emitter and the collector. Thus, fluid flow is generated. A drawback to EHD Ion-Drag pumping is the drop in pumping performance over time. The additional charges introduced to the fluid degrade its overall electrical properties and the emitter electrode loses its high localized electric field at the tip. As a result, the behavior of the fluid electrical properties declines, becoming unsteady, which reduces its efficiency and could pose safety issues [1].

**EHD Induction Pumping**

According to the EHD pumping phenomenon, working fluids initially possess no charge; however, when a high voltage electric field is applied, dipoles are formed. EHD Induction pumping is an EHD flow generation technique, where the flow is based on the dielectrophoretic (DEP) force. It is characterized by a non-uniformity (a gradient) in the electrical conductivity of the working fluid [1]. Given the presence of an interface between liquid and vapor, a temperature gradient, or a specific molecular composition of the fluid, the electrical conductivity within the fluid varies. As a result, an applied AC electric wave attracts and repels those induced charges and, in turn, generates flow. Previously studied applications include enhancing heat transfer of two-phase flow pumping for boiling and condensation as well as liquid film pumping [3].

**EHD Conduction Pumping**

EHD Conduction pumping is a result of dissociated charged particle motion under the effect of a strong electric field within a dielectric working fluid. The dielectric impurities in the fluid separate into charged ions and recombine back into neutrally charged molecules at an equal rate. This equal rate results in overall charge equilibrium. When a high-voltage electric field is applied across an organized set of electrodes placed in the fluid however, much greater amounts of neutral fluid particles exhibit electrolytic properties. Under high-voltage conditions, the rate of dissociation increases, whereas recombination remains relatively constant. Thus, much larger quantities of the fluid experience dissociation and recombination into ions. Consequently, above a critical voltage threshold, the rate of the field-enhanced dissociation is greater than the rate of recombination, which results in non-equilibrium conditions [1].

$$AB \xleftrightarrow[\text{Recombination}]{\text{Disociation/}} A^+ + B^-$$
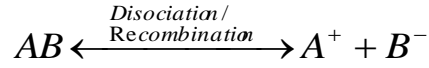
*Figure 1: Molecular Dissociation/Recombination*

As a result, a uniformly charged layer of ions, referred to as the heterocharge layer [1],

forms along each of the electrodes. These heterocharge layers attract to the oppositely charged

electrodes (e.g. positively charged layers draw towards the ground electrodes and negatively

charged layers draw towards the positively charged high voltage electrodes). Since the Coulomb

forces would balance each other if the electrodes were identical in size, the high voltage

electrodes are specifically designed to form drastically larger heterocharge layers and thus create

non-equilibrium forces. As a result, an overall flow is generated, caused by ions dragging fluid

along as they move toward the adjacent oppositely charged electrode. It can be noted that if the

dielectric fluid is purified and remains uncharged, the application of an electric field would not

result in a pumping effect. For the purpose of this study, in single-phase, assuming no change in

temperature, there is no permittivity or density gradient. Thus, the most significant body force

the fluid experiences is the Coulomb force.
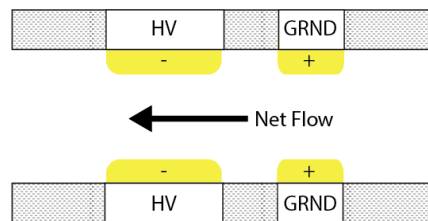


*Figure 2: EHD Pump Electrode Configuration*

The flow of Novec 7600 in this micro-scale EHD pump is entirely based on the EHD

conduction pumping phenomenon. Overall, EHD conduction pumping was chosen over the other

EHD pumping mechanisms due to its high efficiency, durability, and proven efficiency

throughout the experiments and studies done prior to this one.

### 1.2.3 Method of Operation

EHD conduction pumps operate entirely as a result of the EHD conduction phenomenon:

the formation of a heterocharge layer in a dielectric liquid subjected to a high-voltage electric

field. In order to make use of the EHD phenomenon however, the pumps require major design

considerations. Prior research has concluded that precise electrode configuration and positioning

is of utmost importance when attempting to generate flow. Another important detail is the

working fluid selection, often based on the properties of the fluid. In fact, research shows that a

low viscosity, high dielectric constant and low electrical conductivity fluid produces the highest

flow rates with the highest pump efficiency [4]. Specific electrical conductivity of the fluid must

be low (approaching zero, as otherwise, the circuit between the electrodes would be shorted, and

the pump would not function. The last major consideration is the electric field applied to the

fluid. At a low voltage, the critical threshold of the dissociation-recombination cycle would not

be exceeded and an overall flow would not be observed. Under ultra-high voltages however, the

pump electrodes might experience arching due to the high electric field tearing the fluid

molecules apart during fluid breakdown. This results in a spike in fluid conductivity, which in

turn, creates a large current through the fluid medium. In its attempt to ground, the large current

strikes the electrodes, which might result in the electrode melting and physical deformations.

One EHD pump electrode configuration type, used by Feng and Seyed-Yagoobi, is the

perforated disk high-voltage electrode and the ring ground electrode combination [6]. It is an

asymmetric stack up, which includes a perforated disk high-voltage electrode and a ring ground electrode. When voltage is applied, an asymmetric electric field is created, resulting in heterocharge layers along both electrode types. The key difference is in the resultant electric force each charge experiences. The charges formed along the perforated electrode experience a force along the axial direction, while the ring heterocharges experience a force along the radial direction [6]. Thus, a net axial force drives the liquid flow and creates a pressure head.
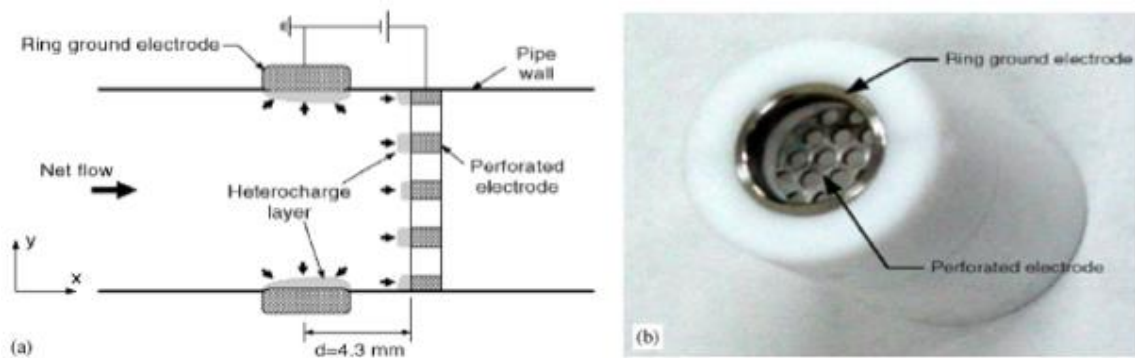


*Figure 3:EHD conduction pump electrode design: (a) schematic and (b) picture from Feng and Seyed-Yagoobi [3].*

Another configuration, used by Patel and Seyed-Yagoobi [3], makes use of an electrode-spacer stack up along two bus lines: a high-voltage carrier and a grounded line. All electrodes have a circular shape and include cutouts for the bus lines and a central hole for fluid flow. The configuration follows a pattern: the high-voltage electrode (a thicker metal piece) is followed by a thin Teflon spacer, which is followed by the grounded electrode (a thinner metal piece), then followed by a thicker Teflon spacer. Electrode spacing is arguably the most important major consideration for EHD pumping, as it directly influences pump operation, behavior, and efficiency. In order to keep the performance of the pump constant, the distance between electrode pairs is always the same. If the electrodes are too close together, the localized electric fields

would be too high, which would result in fluid breakdown. This is explained by the electric field and its direct relation to the imposed voltage across the electrodes and the distance between them. On the contrary, if the electrodes are too far apart, the applied voltages must be very high in order to achieve flow. Hence, the high voltages might pose a safety hazard and additional design constraints. As a general rule, the width of the space between the electrodes is the same as the thinner (ground) electrode. The high-voltage electrode is often designed to be a few times thicker in size compared to the ground [5]. The space in between electrode pair is usually designed to be as much as five times the thickness of the thinner (ground) electrode, so that the electrode pairs do not interfere with each other's electric fields.
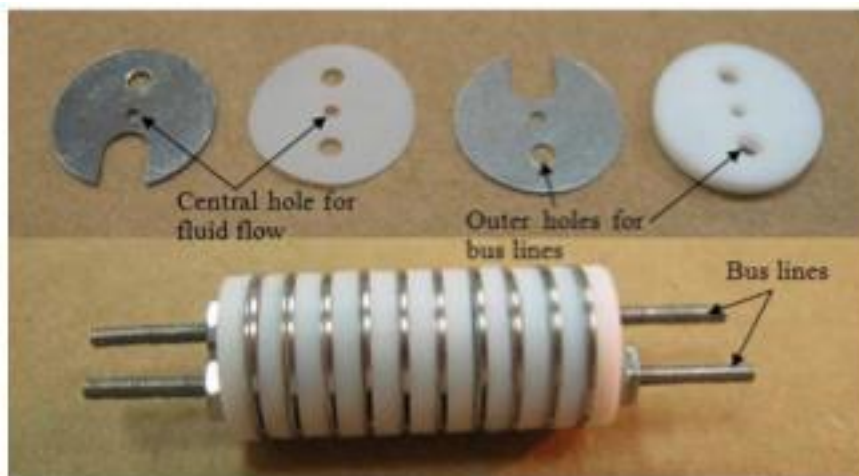


*Figure 4: Electrodes and spacers (top) and assembled EHD pump (bottom) with 10 electrode pairs*

A variety of electrode configurations could be designed following the major design considerations: electrode positioning and configuration, working fluid selection, and magnitude of voltage to be applied. Those configurations result in measurable output, such as flow rate and pressure drop across the pump or flow channels. With EHD conduction pumping systems, the number of electrodes in series corresponds to the achievable magnitudes of pressure drop and flow rate performance increasing it nearly linearly [3].

**1.4 Potential Applications**

There are a number of advantages to EHD conduction pumping with regards to mass transport (control and distribution) and efficient heat transfer. Most industrial applications include a special constraint, which has to be overcome by controlling the liquid flow in order to enhance heat transfer.

The major advantage to EHD pumping is its flexibility. The EHD conduction pumping phenomenon is responsive, i.e. pumping changes almost instantaneously when changing the imposed electric field [1]. EHD pumps have a simplistic and light design, as well as no moving parts, which makes them both silent and ideal for environments beyond human reach (Earth orbit or micro-scale applications). The phenomenon is applicable to both single and two-phase flow [1]. Since the current is low (in the mA), when supplied with voltage (in the kV), EHD pumps have a significantly lower power consumption compared to traditional mechanical pumps. Most working fluids in thermal systems happen to be dielectrics, which makes flow distribution and control using EHD conduction pumps entirely achievable.

The major disadvantage to EHD conduction pumping is the requirement of a high voltage electric field supply, which poses risks and overall system design constraints.

One particular application is in weightless environments, where the scarcity of gravity and human reach overall requires dependable technology and, preferably, no moving parts. Similarly, in a standard refrigeration cycle, the two-phase working fluid undergoes heat transfer in the form of condensation and evaporation, the efficiency of which could be greatly improved [Viral]. In some forms of cooling for instance, the working fluid could be redistributed to match

local heat transfer needs and preserve efficient system operation. EHD pumping is a modern age field of study and research has not fully explored its full capabilities yet.

## 1.5 Previous Experiments

Previous efforts to characterize EHD flow distribution and pressure generation have resulted in a variety of experiments designed to determine the effect of EHD conduction both analytically and empirically. Feng and Seyed-Yagoobi [6] have investigated single and two-phase flow control utilizing EHD conduction pumping in two parallel pipe channels. These experiments resulted in effective control of flow distribution in both liquid and vapor phase between channel lines. Patel and Seyed-Yagoobi [3] have investigated single-phase flow along a single channel.

The results from previous studies proved the ability to control single and two-phase flow in single and two branch piping configurations. Feng's [6] work focused on establishing control of two-phase distribution between two branch lines, while Patel's [3] work showed desirable pressure and flow generation in single-phase. Patel [3] confirmed flow generation of up to 7 cm/s and a low power requirement (0.2 W) for the micro-scale EHD pump in a meso-scale tube setup.

This study is a continuation of the work done by Feng, Patel, and Seyed-Yagoobi. The micro-scale EHD conduction pump used by Patel has been implemented due to its reliability. The equipment in the flow control loop assembled in this experiment can be used for future work in two-phase flow.

### 1.5.1 Control of Liquid Flow Distribution Utilizing EHD Conduction Pumping

Feng concluded that the flow distribution among the channels is somewhat analogous to the electric current distribution in a parallel circuit [6]. The mass conservation law states that the

the sum of mass flow entering each branch should be equal to the total flow rate. Therefore, flow

rate for branch 1 can be calculated from measurement:

$$\dot{m}_1 = \dot{m}_{total} - \dot{m}_2 - \dot{m}_3$$

From the Darcy–Weisbach equation, the pressure drop along the pipe flows can be

expressed as

$$\Delta P = f \frac{\dot{m}}{2\rho\left((\pi/4)D^2\right)^2} \frac{L}{D}$$

where

$$f = \frac{64}{\mathrm{Re}} = 64 \frac{\rho L u_{mean}}{\mu}$$

for Re<2300. If the total mass flow rate remains constant and $\Delta P_{EHD}$ varies with the pressure head

generated by EHD pumps, the relationship between mass flow rate and EHD pumping pressure

can be expressed as

$$f_1 \frac{\dot{m}_1}{2\rho\left((\pi/4)D_1^2\right)^2} \frac{L_1}{D_1} - \Delta P_{EHD} = f_2 \frac{\dot{m}_2}{2\rho\left((\pi/4)D_2^2\right)^2} \frac{L_2}{D_2} = f_3 \frac{\dot{m}_3}{2\rho\left((\pi/4)D_3^2\right)^2} \frac{L_3}{D_3},$$

assuming that the pressure drops along each branch channel are identical. If the length and

diameter of each channel is kept identical, the equation could be simplified to

$$\Delta P_{EHD} = f \frac{\dot{m}_1 - \dot{m}_2}{2\rho\left((\pi/4)D^2\right)^2} \frac{L}{D} = f \frac{\dot{m}_1 - \dot{m}_3}{2\rho\left((\pi/4)D^2\right)^2} \frac{L}{D},$$

which implies a linear relationship between pressure generation from EHD pumps and flow rate

difference in branch channels.

## Chapter 2: Methodology and Experimental Setup

### 2.1 Overview

The purpose of this series of experiments was to investigate the flow distribution capabilities of EHD conduction driven systems, which includes applications such as misdistribution correction, interchannel control, and intentional channel draining. Specifically, the experiments were designed with the intention of determining the power inputs required for each of the pumps to both correct and cause maldistribution in the other channels. Also an important focus was to determine the amount of power needed for one or more of the pumps to drain the remaining channel(s). In order to accomplish these goals, the following task specifications were developed to allow for adequate phenomena exemplification and system study:

- The experiments must display the flow distribution characteristics of as many pumping configurations as possible. This includes the control of one channel's flow using two pumps, the control of one channel's flow using one pump with the third channel closed to flow, and so on.

- The experiments must produce meaningful data. This is accomplished through appropriate measurement device positioning, device calibration, programming logic, and data post-processing.

- The system must be controllable through LabVIEW Virtual Instrumentation software. Considering LabVIEW was the most applicable and available software and that similar experiments have been performed using this same software, this is appropriate for the purposes of consistency and simplicity.

- The applied EHD voltages must be able to produce pressures and flow rates that are measurable above the main flow produced by the mechanical pump. Due to the integration of multiple scales within the same system, the meso-scale pumps must be able to produce measurable results considering that they are the main focus of this series of experiments. Additionally, the system must be built to accommodate the amount of pressure that the EHD pumps can generate. Larger systems may contain pressure drops that are too large for the EHD pumps to overcome, leading to negligible changes and immeasurable results. For this reason, the pressure drops in the system were reduced using larger diameter tubes outside of the EHD pumps.

In order to test the full scope of options regarding EHD pump application, this series of experiments involves three meso-scale EHD pumps in parallel channel configuration, which is a system configuration that has not yet been investigated. This particular setup will provide the level of insight necessary to design and examine any EHD pumping configuration that may involve multiple pumps and channels.

For our chosen configuration, pressure transducers, flow meters, and power sensors were used to determine the pumping capabilities of each of the system components. LabVIEW virtual instrument programs and National Instruments data acquisition boards were used as user interfaces for measurement, control, and data management purposes. These systems, combined with the system of sensors, allow for the study of the EHD flow distribution capabilities by allowing one to acquire quantitative data on pressure and flow generation as a function of input electrical power. This particular relationship is, in part, the focus of the series of experiments;

from here, one is able to determine the relationship between user input power and the pumps'

abilities to control flow throughout the system.

**2.2 Physical Components**

The most notable components operating within the experimental setup were the three

meso-scale EHD pumps and the upstream mechanical pump. The three meso-scale pumps were

in parallel configuration and the mechanical pump was positioned upstream in order to drive the

majority of the flow in the parallel lines. Once adequate flow was achieved in the system by the

mechanical pump, the flow in each branch line was adjusted through use of both needle valves

and the meso-scale EHD pumps depending on the desired outcome for each experiment. For

example, in the latter experiments performed the needle valves in each branch line were used to

intentionally maldistribute flow such that the correction capabilities of the micro-scale EHD

pumps could be examined. Additionally, various flow sensors, differential pressure transducers,

and voltage/current monitors were used either in series (in the cases of the flow sensors) or in

parallel (in the cases of the pressure transducers and the power monitors) with the flow of the

system. The system configuration can be seen below.
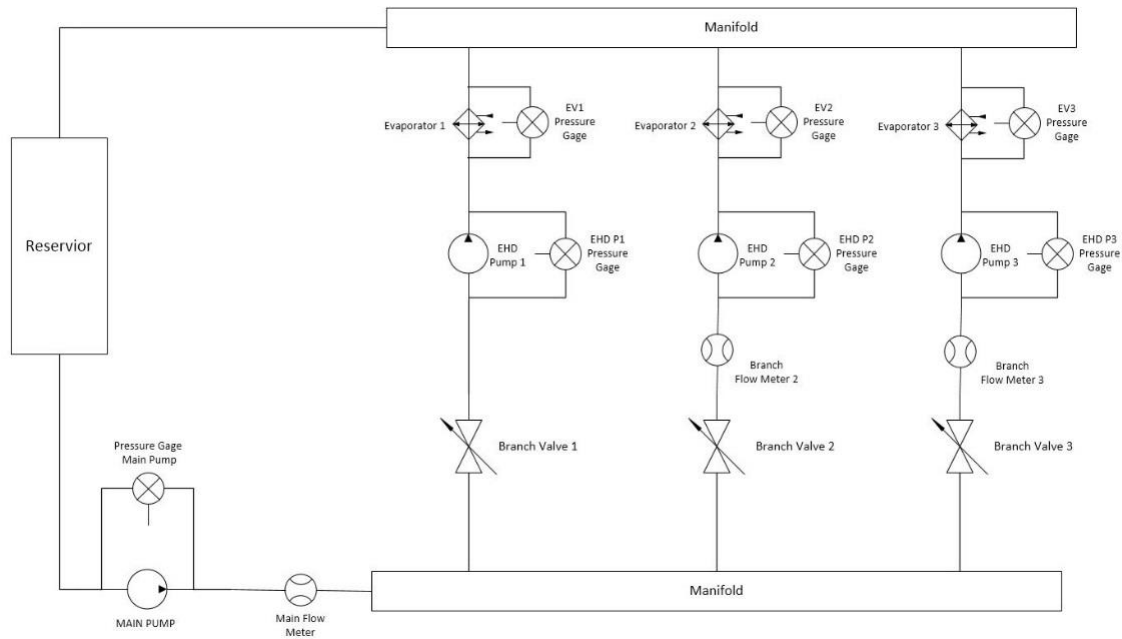
*Figure 5: Diagram of 2-Scale EHD Pumping System Configuration*

Also included is a photograph of the final experimental setup. It can be seen that the evaporator lines and pressure transducers (shown in the red box on the photograph) were not included in the previous diagram. This is because they had no effect on the experiments that were performed other than adding internal volume. Additionally, the evaporator pressure transducers were not activated for the experiments performed. Additional sections and devices, however, come to play a role in the future adaptation of the system to two-phase flow.
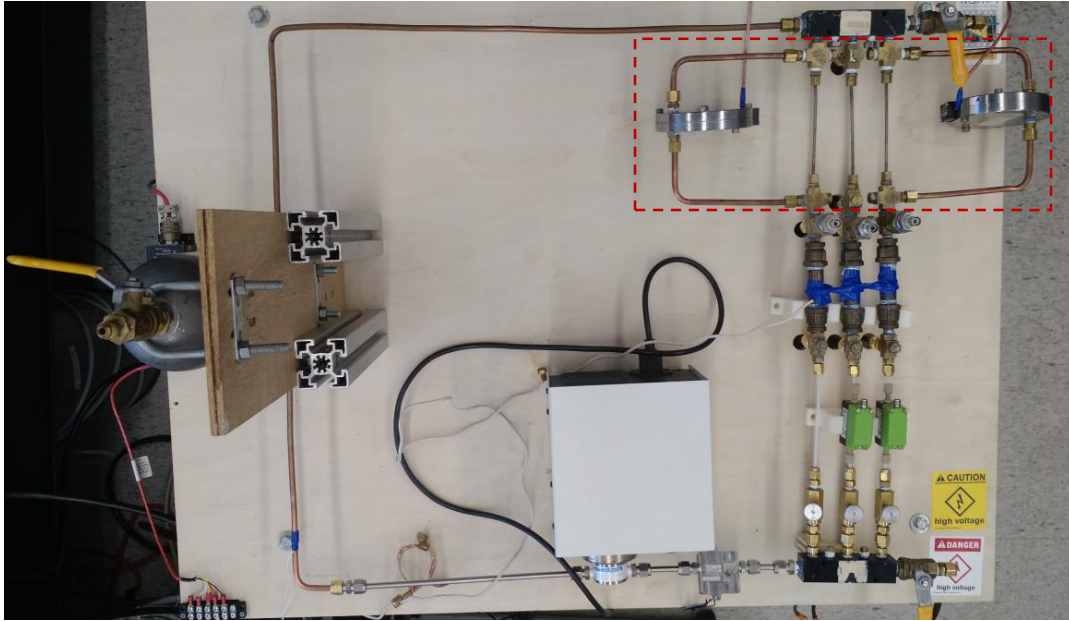
*Figure 6: Photograph of EHD Pumping System Configuration*

### 2.2.1 In-Line Loop Components

The most influential apparatus used in this series of experiments was the meso-scale mechanical pump. More specifically, a Cole-Parmer Model 75211-10 50-5000 RPM 0.07HP mechanical pump was used to produce overall system flow rates of between 5 mL/min and 30 mL/min. This pump can be seen in Figure 3 below.
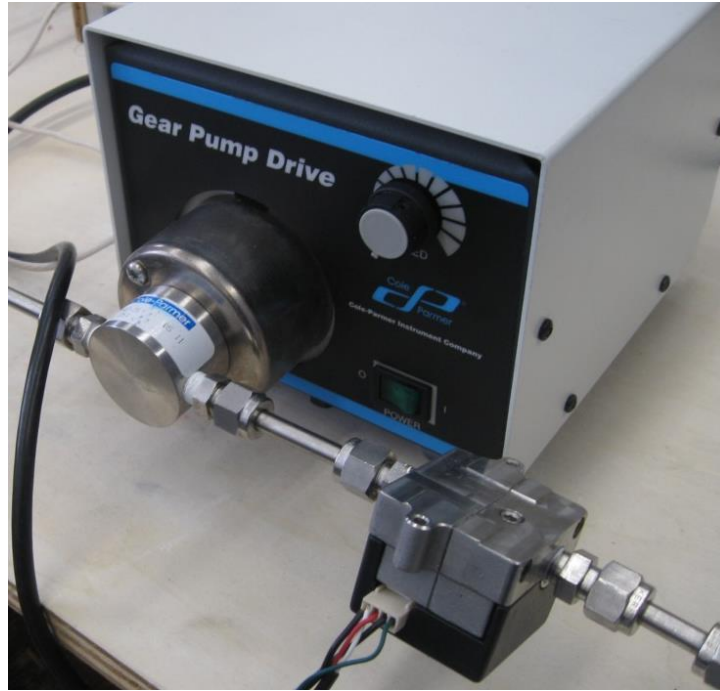
*Figure 7: Cole Parmer Model 75211-10 Mechanical Pump*

This generated flow was fed directly into a manifold that will effectively be considered a reservoir for analysis purposes. This manifold consists of a ¼ inch-diameter fluid intake and three 1mm-diameter exit channels (as seen in Figure 4). Due to mass conservation:

$$\dot{m}_{IN} = \dot{m}_1 + \dot{m}_2 + \dot{m}_3$$

where $\dot{m}_{IN}$ is the flow rate into the manifold, $\dot{m}_1$ is the flow rate out through Channel 1, $\dot{m}_2$ is the flow rate out through Channel 2, and $\dot{m}_3$ is the flow rate out through Channel 3. The volume of the manifold is significant, as it stores a certain volume of fluid before outputting flow into each branch line. This effect is also incredibly significant to the flow control of each branch line, which will be seen later in this report.
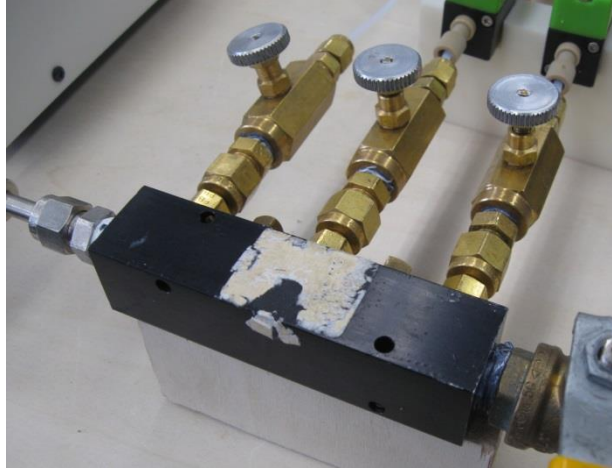
*Figure 8: Distribution Manifold Assembly*

Each of the three branch lines consisted of mechanical needle valves, plastic and copper

piping, and the three EHD pumps studied. The needle valves were positioned closest to the

manifold outputs such that flow into each individual line could be modified. In this study,

intentional maldistribution was introduced using these valves, which could be closed to a certain

degree to reduce flow that would be subsequently corrected using the EHD branch pumps.

Additionally, many of the experiments conducted concerned one or two of the branch lines. For

example, multiple experiments were performed where the flow control characteristics of two

channels using one pump were examined. In these cases, one of the branch lines was closed

entirely using the needle valve. This same technique was used when examining the individual

performances of each of the pumps. Following the valves in Channels 2 and 3 were Sensirion

Model SLQ-HC60 flow sensors (which will not be discussed further in this section). Channel 1

did not require a flow sensor, as its flow could be determined through knowledge of the flows in

the other two lines and the overall flow produced by the mechanical pump. This was

advantageous due to the high costs associated with the branch flow sensors. Since Channel 1 did

not contain a sensor a longer plastic tube was used at the outlet of the manifold to Channel 1.

Between these sensors and the adjacent components were 1mm-diameter plastic tubes, which

were required due to the interfaces of the flow sensors. The tubes that either followed the sensors

(in Channels 2 and 3) or the manifold (in Channel 1) were then fed into each of the 3 micro-scale

EHD pumps. Considering the entire pump assemblies consisted of copper, plastic-to-metal

interfaces did exist at the inlets to each of the pumps. Although this was undesirable, it was

necessary and advantageous due to the desire for the accuracy and precision provided by the

Sensirion flow sensors. The micro-scale pumps, when activated through varying voltage

application, increased or decreased flow and pressure in each of the branch lines according to the

desired study. An image of the system pump assembly can be seen in Figure 5.



*Figure 9: Micro-scale EHD Pump Configuration*

Following the EHD pumps was a second manifold (again, considered a reservoir for all

intents and purposes) that merged the flow in the branch lines back into a single main line (seen

in Figure 6).
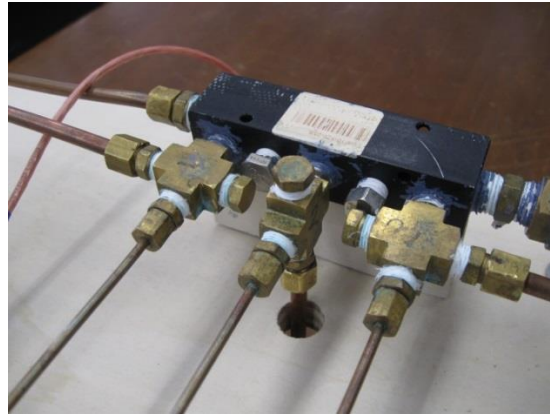
*Figure 10: Merging Manifold Assembly*

The final component in the loop was the actual fluid reservoir (see Figure 7), which was positioned vertically and left open to the system in order to ensure not only that the fluid permeated throughout the system, but also to ensure that any fluctuation in fluid volume within the loop due to temperature variation would cause the reservoir to fill rather than causing the loop hardware to expand. The outlet port of the reservoir interface was then input back into the mechanical pump, completing the loop.



*Figure 11: Fluid Reservoir Assembly*

Finally, the working fluid in the system was 3M Novec HFE-7600. This particular fluid was chosen due to its properties under the applied pressure as well as its dielectric properties, which allow it to dissociate under high-voltage electric fields (the driving principle behind EHD conduction pumping). A specifications sheet of its physical properties is attached in Appendix A.

### 2.2.2 Measurement Equipment

As mentioned previously, various series and parallel components were used to make the appropriate quantitative measurements such that the effects of the EHD pumps on the individual branch flows and pressures could be understood. Referring to the previous loop description, a main flow meter (seen in Figure 3) was installed following the mechanical pump such that the flow in Channel 1 could be calculated without the use of an additional branch flow sensor. Moving to the region after the needle valves, a Sensirion Model SLQ-HC60 Liquid Flow Sensor was installed in Channels 2 and 3 to accurately measure the flow induced in each of these two branches. These sensors can be seen in Figure 8. Considering that these were placed directly adjacent to the EHD pumps, the pressure drop between the branch flow sensors and the EHD pumps was negligible, providing further accuracy to the flow readings. Differential pressure transducers (depicted below) were positioned in parallel with each of the EHD pumps to measure their respective pressure generations. The calibration curves of both the flowmeters and the pressure transducers are attached in Appendices C and D.
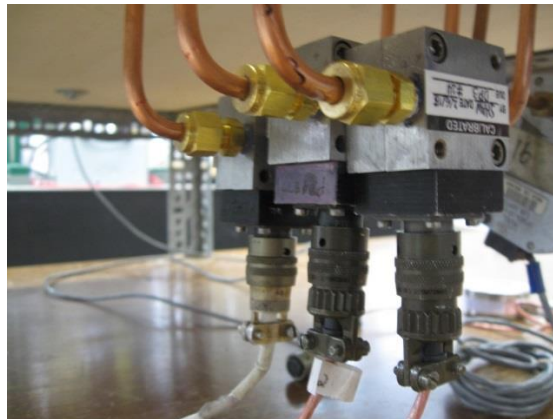
*Figure 12: Undermounted EHD Differential Pressure Transducers*

### 2.2.3 External Components

The system control was interfaced through LabVIEW Visual Programming and Instrumentation Software in conjunction with both a National Instruments SCB-68 Data Acquisition Module and a National Instruments USB-6009 Data Acquisition Module. Two separate DAQ boards were used for this series of experiments due to a need for one user output and eight system inputs. The chart below outlines the port configurations for all system measurements taken. Additionally the second board was installed in anticipation for the adaptation of the system to two-phase flow and an additional meso-scale EHD pump, which would require additional voltage and current monitors, user outputs, and differential pressure gauges. Images of both of the data acquisition modules can be seen in Figures 9 and 10 following the chart.

*Table 1: Data Acquisition Configuration for EHD Pumping Experimental Measurement*

| MEASUREMENT | DAQ BOARD | PORT |
|---|---|---|
| Applied EHD Voltage(V123) | NI SCB-68 | AO-0 |
| Voltage Monitor (VReal123) | NI USB-6009 | AI-0 |
| Current Monitor (C123) | NI USB-6009 | AI-1 |
| Channel 1 EHD Differential Pressure Generation (DP1) | NI SCB-68 | AI-1 |
| Channel 2 EHD Differential Pressure Generation (DP2) | NI SCB-68 | AI-2 |
| Channel 3 EHD Differential Pressure Generation (DP3) | NI SCB-68 | AI-3 |
| Total System Flow Generation (FRM) | NI USB-6009 | AI-2 |
| Channel 2 Flow Generation (FR2) | NI USB-6009 | AI-3 |
| Channel 3 Flow Generation (FR3) | NI USB-6009 | AI-4 |
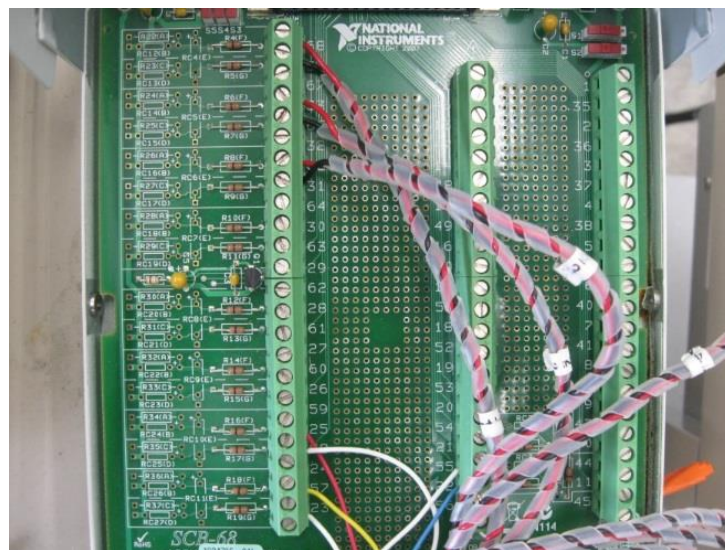


*Figure 13: NI SCB-68 Data Acquisition and User Output Configuration*

*Figure 14: NI USB-6009 Data Acquisition Configuration*

A LabVIEW virtual instrumentation interface was developed to obtain and process the

input values (all of which were voltage readings, output from their respective sensors and

gauges, ranging from 0V to 10V) into more realizable and useful readings. For example, an input

voltage from a pressure transducer may read 5V, but in order for that information to be useful it

must be processed through internal LabVIEW logic. Following calibration of the transducer, the

reading on the instrumentation interface may measure about 300Pa when the input from the

transducer measures 5V. All measurements and outputs were similarly calibrated and processed

to provide the desired results. The LabVIEW interface used for the experiments can be seen

below. Included in Appendix E is the detailed Block Diagram for this virtual instrument panel.



*Figure 15: LabVIEW Virtual Instrumentation Front Panel*

An existing power box was built to provide the high voltages needed to operate the three EHD pumps. This power pox (depicted in Figure 12) consists of four switches (one for each of the EHD pumps and one for the box as a whole) and a transformer to convert the wall power supply (120V$_{RMS}$ AC) into usable power.
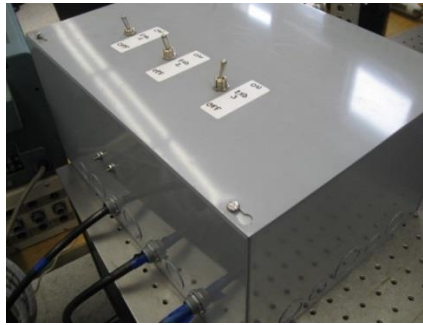


*Figure 16: Power Supply to EHD Pumps*

Due to the nature of the transformer, all of the voltages output from the box must be equal. For example, if a signal is received by the box from LabVIEW that indicates the box should apply a voltage of 1kV, all three of the outputs to the pumps will receive 1kV. For this reason, the individual channel switches were installed such that one or two of the pumps could be turned off while a voltage is applied to the other channel(s). The switching configuration can be seen more clearly in Figure 13.
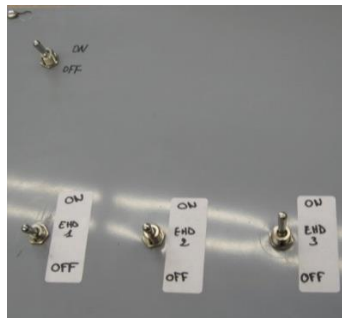


*Figure 17: Power Box Switching Setup*

Lastly, EHD Pump mounts and flow sensor mounts were rapid prototyped to provide stability for the pumps and ensure system linearity. This is vital to the future modification of the system to adapt it to two-phase flow, as the loop's height must remain constant to avoid internal vapor pressure losses and ensure accurate measurements. The schematics for these mounts can be seen in Appendices B-1 and B-2.

## 2.3 Experimental Matrix

### 2.3.1 Initial Conditions and Ranges

A set of boundary values were assigned to several parameters according to different limitations. These parameter limits are described below.

The flow rate in each branch should be between 1-15ml/min. This was affected by the measurability of flow meter, pressure generation of the main pump, and pump performance of each individual branch pumps, because the flow meter in each pump could measure up to 50 mL/min. The main pump was able to provide each branch line with consistent flow rates of up to 20 mL/min, and each EHD pump in branch line could produce maximum flow rate increase of about 3 mL/min. Therefore, to generate consistent flow as well as to ensure no overflow occurs in the branch lines, the lower limit was set to 1 mL/min and the upper limit was set to 15 mL/min.

Due to hardware limitations, the operating voltages in each EHD pump should fall between 0-1500V. From previous tests, it was proven that the EHD pumps worked best at 1500V, but increasing the voltage any higher could result in sparks in the pumps and would lead to potential

failure due to fluid break down. For these reasons, the range of the voltage was set to a maximum if 1500V.

Maximum pressure differences in each branch line was found to be 1200Pa based the calibration curves of the pressure transducers.

### 2.3.2 Experimental procedures

**Voltage Stepping and Measurement Cycles**

All the experiments would require taking data sets at each level of EHD pump voltages, with the voltage increasing from 0V to 1500 V, decreasing back from 1500 to 0V, and going up to 1500V the back down again, with a increment of 100V every time.

The stepping was to guarantee that in each measurement, steady state was achieved, which allowed the pump performance to settle between each voltage increase and therefore avoid transient effects. The stepping also ensured safety, since it could provide enough time for the team to identify whether there exist a sound of spark.

One experiment data sheet would include two cycles that repeats same processes. The purpose of cycling was to assure the repeatability of experiments.

**Data Recording**

The data taken from the experiment included: the voltage of EHD pump in each branch line, the current of EHD pump in each branch line, the flow rate and pressure difference in each branch line.

Before taking the data, a settling time of approximately 30 seconds was allowed. Then the

values were taken every second for consecutive 20 seconds, and would be averaged for later analysis.

### 2.3.3 Experiment I: Individual Pump Performance

In the test for individual pump performance, only the valve in the branch line being tested was fully open, the other two were closed. The main pump was turned on to provide certain flow rate, and the EHD pump in the corresponding branch line was then turned on, with voltage increasing from 0-1500 V. The test was repeated at different overall flow rate level, and for EHD pumps in branch 2 and 3.

*Table 2: Experiment matrix for individual pump performance*

| Overall Flow Rate [mL/min] | Valve 2 | Valve 3 | Pump 2 | Pump 3 |
|---|---|---|---|---|
| 1.5 | Closed | Open | Inactive | Active |
| 1.5 | Open | Closed | Active | Inactive |

Existing work for pump performance at different voltage and flow rate level is presented in the picture below:
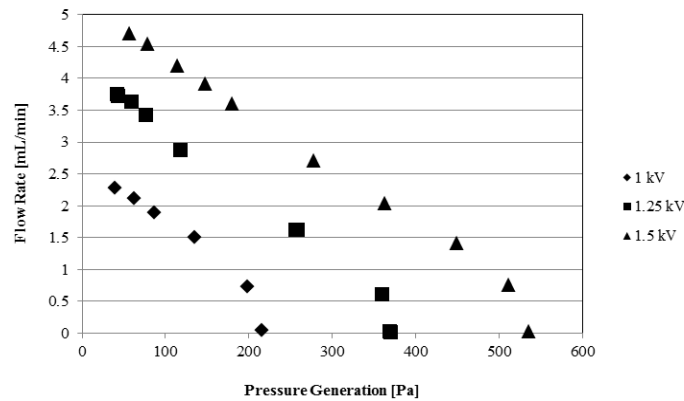


*Figure 18: EHD Pump Performance Curve*

### 2.3.4 Experiment II: Even Flow Distribution to Forced Maldistribution

This experiment sought to test the draining effect on branches by operating individual pump other branches, and was divided into two cases: two branches open, and three branches open.

In the first case, Valve 1 was kept closed in these set of experiments, so that only flow rates in branch 2 and branch 3 were studied. After the main pump was turned on at a desired total flow rate, the valves for branch 2 and 3 were adjusted so that the flow rates in both branches became equal. Then the EHD pump in branch 3 was turned on, with increasing voltage up until 1500V, going back to 0V, and repeated. Data were take every 100V increment. Similarly, the same test was performed with only EHD pump in branch 2 turned on. This experiment was iterated with different total flow rate provided by the main pump.

*Table 3: Experiment Matrix for: Even Flow Distribution to Forced Maldistribution, Case I*

| Overall Flow Rate [mL/min] | Flow Rate 2 [mL/min] | Flow Rate 3 | Valve 1 | Valve 2 | Valve 3 | Pump 1 | Pump 2 | Pump 3 |
|---|---|---|---|---|---|---|---|---|
| 10 | 5 | 5 | close | close | open | close | inactive | active |
| 10 | 5 | 5 | close | open | close | close | active | inactive |
| 15 | 7.5 | 7.5 | close | close | open | close | inactive | active |
| 15 | 7.5 | 7.5 | close | open | close | close | active | inactive |
| 20 | 10 | 10 | close | close | open | close | inactive | active |
| 20 | 10 | 10 | close | open | close | close | active | inactive |

In the second case, all three branches are open and the valves for Branches 1, 2 and 3 were adjusted so that the flow rates in both branches became equal. Then the EHD pump in both

branch 2 and 3 was turned on, with increasing voltage up until 1500V, going back to 0V, and

repeated.

Table 4: Experiment Matrix for Even Flow Distribution to Forced Maldistribution, Case II

| Overall Flow Rate [mL/min] | Flow Rate 1 [mL/min] | Flow Rate 2 [mL/min] | Flow Rate 3 [mL/min] | Valve 1 | Valve 2 | Valve 3 | Pump 1 | Pump 2 | Pump 3 |
|---|---|---|---|---|---|---|---|---|---|
| 19 | 3.5 | 3.5 | 3.5 | Open | Open | Open | Inactive | Active | Active |

The expectation for this experiment was to see that increasing in EHD pump voltage in

one branch would result in pressure change in its corresponding pressure difference, and

therefore enhance the flow rate by draining the other branch, while the overall flow rate is

maintained approximately the same.


### 2.3.5 Experiment III: Maldistribution to Even Flow Distribution

This experiment sought to test the controllability in flow rate using EHD pumps, and was

divided into two cases: one branch controls another one, and two branches control the third one.

In the 'one branch controls another one' case, valve 1 was kept closed. After the main

pump was turned on, valves were adjusted to yield unequal flow rate in branch 2 and 3, with

branch 3 less 2 by approximately 1 ml/min. Then the EHD pump in branch 3 was turned on, with

increasing voltage up until 1500V, going back to 0V, and repeated. Data were take every 100V

increment. Similarly, the same test was performed with branch 2 less 3 by approximately 1

ml/min and only EHD pump in branch 2 turned on. This ensnarement was iterated with different

total flow rate provided by the main pump.

*Table 5: Experiment Matrix for Maldistribution to Even Flow Distribution, Case I*

| Overall Flow Rate [mL/min] | Flow Rate 2 [mL/min] | Flow rate 3 [mL/min] | Valve 1 | Valve 2 | Valve 3 | Pump 1 | Pump 2 | Pump 3 |
|---|---|---|---|---|---|---|---|---|
| 10 | 5.5 | 4.5 | close | close | open | inactive | inactive | active |
| 10 | 4.5 | 5.5 | close | open | close | inactive | active | inactive |
| 15 | 8 | 7 | close | close | open | inactive | inactive | active |
| 15 | 7 | 8 | close | open | close | inactive | active | inactive |
| 20 | 10.5 | 9.5 | close | close | open | inactive | inactive | active |
| 20 | 9.5 | 10.5 | close | open | close | inactive | active | inactive |

In the 'two branches control the third one' case, all valves are open, and were adjusted so that branch 2 and 3 share same flow rate, but both less branch 1 than 1 ml/min. Then the EHD pump in branch2 and 3 was turned on, with increasing voltage up until 1500V, going back to 0V, and repeated. Data are take every 100V increment.

*Table 6: Experiment Matrix for Maldistribution to Even Flow Distribution, Case II*

| Overall Flow Rate [mL/min] | Flow Rate 1 [mL/min] | Flow Rate 2 [mL/min] | Flow Rate 3 [mL/min] | Valve 1 | Valve 2 | Valve 3 | Pump 1 | Pump 2 | Pump 3 |
|---|---|---|---|---|---|---|---|---|---|
| 19 | 7 | 6 | 6 | open | open | open | inactive | active | active |
| 19 | 6 | 7 | 6 | open | open | open | active | inactive | active |
| 19 | 6 | 6 | 7 | open | open | open | active | active | inactive |

However, due to the unstable power output in branch 1 from power box, experiments that would use EHD pump1 were eliminated.

Furthermore, due to the construction structure of the power box, when both EHD pump 2 and 3 were on, they shared the same voltage.

The expectation for this experiment is to see that increasing in EHD pump voltage in one branch or two branches would result in pressure change in its corresponding pressure difference,

and therefore enhance the flow rate. Eventually, even flow distribution should be acquired by adjusting the voltage on each EHD pumps.

**Chapter 3: Results and Discussion**

**Experiment I: Individual Pump Performance**

In order to establish the EHD pumping behavior in each branch line, a thorough analysis of the flow rate and pressure generation capabilities of each pump was required. The flow rate vs. applied voltage and pressure vs. applied voltage characteristics were obtained for the pumps in Branches 2 and 3. The abilities for the individual EHD Pumps to generate flow under certain applied voltages were investigated by closing off flow in the remaining channels and measuring the flow generated in the channel in question. For example, in order to measure the ability for EHD Pump 3 to generate flow under certain applied voltages, Channels 1 and 2 were closed off and measurements were taken via the flow sensor and the pressure transducer in Channel 3. The curve for EHD Pump 3 can be seen below with applied voltage iterations of 100V.
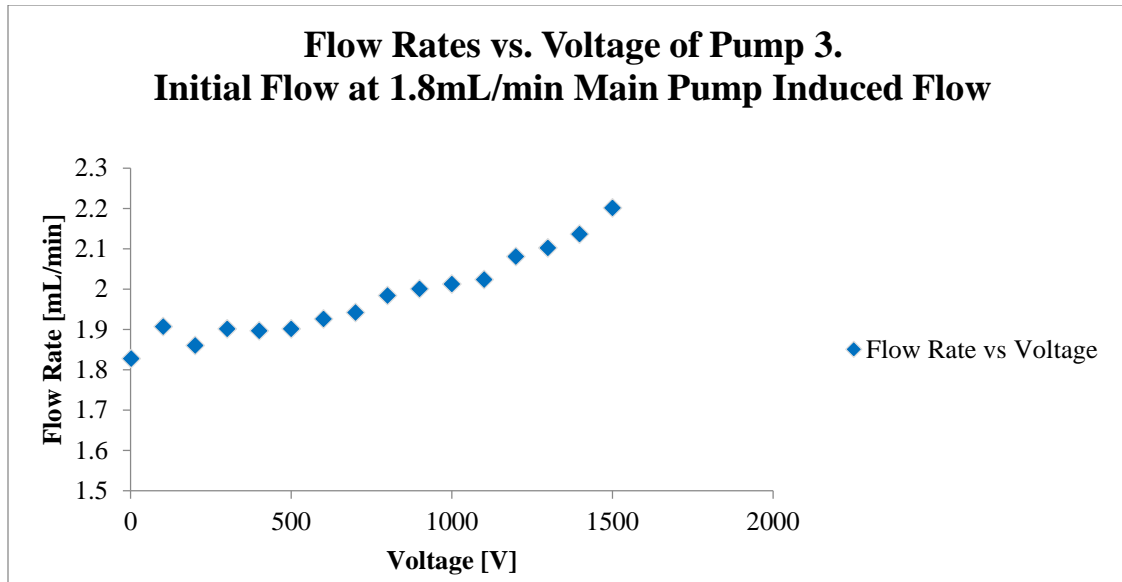
*Figure 19: Flow Rate Generation Characteristic of EHD Pump 3*

According to Figure 17, increasing the voltage results in an increased flow rate. This proves the

EHD conduction phenomenon. There is a slight error in the second measurement, possibly

caused by the instability in supply of flow rate by the mechanical pump.
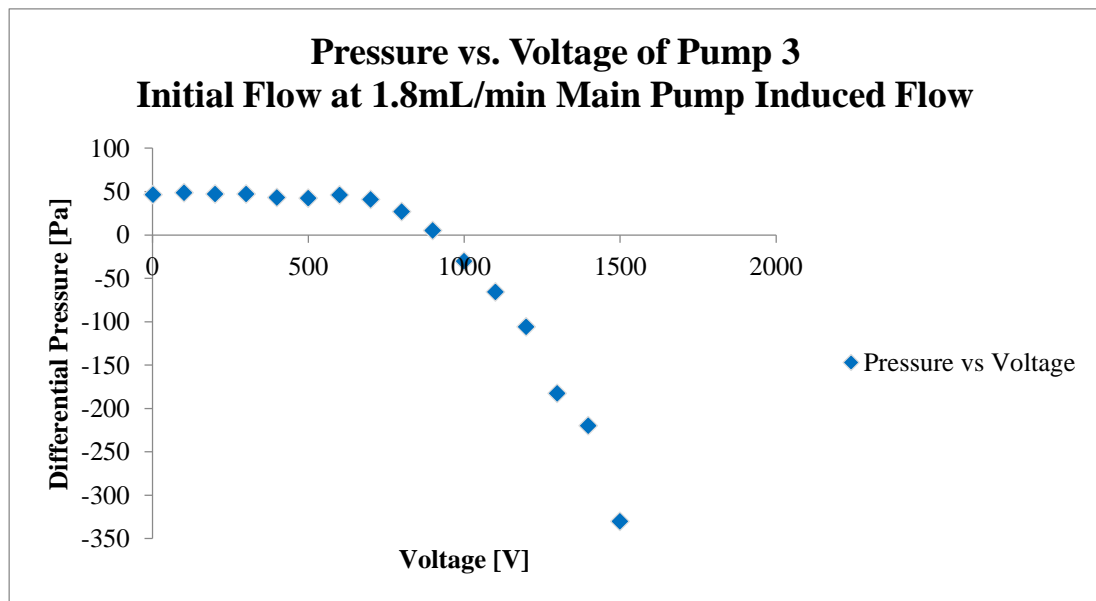


*Figure 20: Pressure Generation Characteristic of EHD Pump 3*

According to the graph, increasing the voltage results in a drop of pressure across the pump. The pressure generation behavior matches the flow rate behavior from the previous graph. It also matches the study conducted by Pearson and Seyed-Yagoobi describing the EHD pump characteristic shown in Figure 16. Thus, the negative pressure drop of 380Pa shown in Figure 18 corresponds to an active EHD pump generating pressure.

The behavior of the two EHD pumps was established to be comparable, with EHD Pump in Branch 2 being less effective with regards to pressure generation. The pressure vs. voltage characteristics of EHD Pump 2 is displayed in the graph below.



*Figure 21: Pressure Characteristic of EHD Pump 2*

The overall pressure drop in the EHD Pump in Branch 2 is about 300Pa. Compared to the pressure drop generated by the EHD Pump in Branch 3 (380Pa), we can conclude that EHD Pump in Branch 2 is 25% less effective.

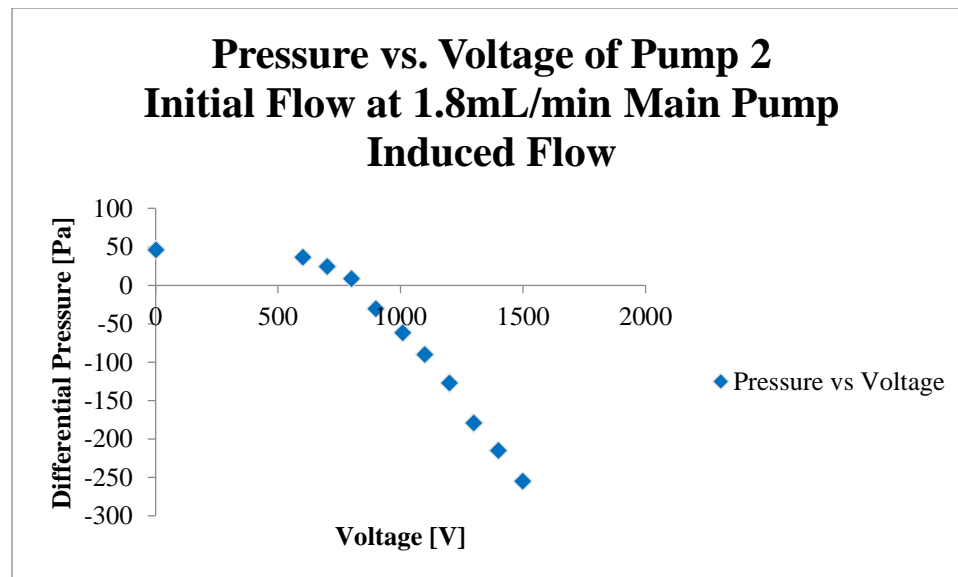**Experiment II: Even Flow Distribution to Forced Maldistribution**

### A. Two Branch Experiments

For the experiment regarding creating forced maldistribution from an even flow in two

parallel branches, inactive channel 2 and active channel 3 were utilized. Channel 1 was kept

closed, while the mechanical valves on Channels 2 and 3 were initially adjusted to equalize their

flow rate. The purpose of this experiment was to investigate the capabilities of the EHD pump in

Channel 3 to generate increased flow in order to induce an increased flow rate in channel 3 and

observe a reduction in flow rate in channel 2 due to conservation of mass, considering a constant

flow rate entering the distributing manifold. The following plot demonstrated the results obtained

when the above configuration is utilized and the applied voltage to EHD Pump 3 is increased in

increments of 100V per minute, peaking at 1500V and decreasing back to zero in a similar step-

size fashion. This was repeated twice to assure continuity and to obtain results that were

sufficient for analysis. The flow generated by the main mechanical pump was held constant at

11mL/min. An additional plot with an overall induced flow rate of 3.2mL/min can be seen in

Appendix F.

*Figure 22: Flow Maldistribution Characteristics of EHD Pump 3 on Inactive Channel 2*

The plot shows that at the maximum applied voltage, the EHD Pump in Channel 3 is able to create a flow rate difference of 1mL/min. It can also be seen that at applied voltages of about 0V, the flow rate in both channels 2 and 3 is equal, much like their initial values. It is also important to note that the overall flow rate changes insignificantly throughout the experiment.

The next plot presents the pressure across each branch plotted against time. The graph yields that active Branch 3 generates a higher pressure drop compared to the inactive Branch 2 when subjected to high voltage.
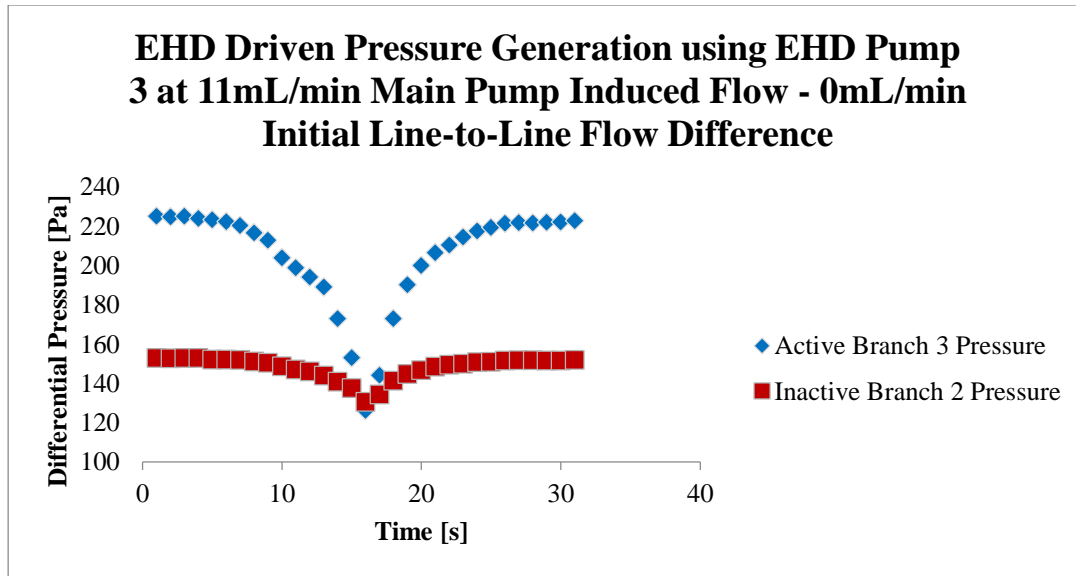
*Figure 23: Maldistribution Pressure Generation Characteristics of EHD Pump 3 on Inactive Channel 2*

In conclusion, the EHD conduction pumping phenomenon is present and functions effectively in meso-scale pumping.

### B. Three Branch Experiment

For the final experiment, the intentional maldistribution capabilities of the three-channel system were investigated when all three channels were opened and two of the pumps were activated. More specifically, EHD Pumps 2 and 3 were activated while Branch 1 was left open and EHD Pump 1 remained inactive. Before applying voltages to EHD Pumps 2 and 3, a main flow was introduced by the mechanical pump and the flows in each of the three branch lines were equalized using the mechanical needle valves. From there, the voltages in EHD Pumps 2 and 3 were increased from 0V to 1500V in iterations of 100V per minute. Due to mass conservation in the manifold it can be assumed that increasing the flows in Channels 2 and 3 (through increasing the applied voltages) will decrease the flow in Channel 1.

The following plot demonstrates the results obtained when the above configuration was utilized and the applied voltages to EHD Pumps 2 and 3 were increased simultaneously in increments of 100V per minute, capping out at 1500V. The flow generated by the main mechanical pump was held constant at 10mL/min.
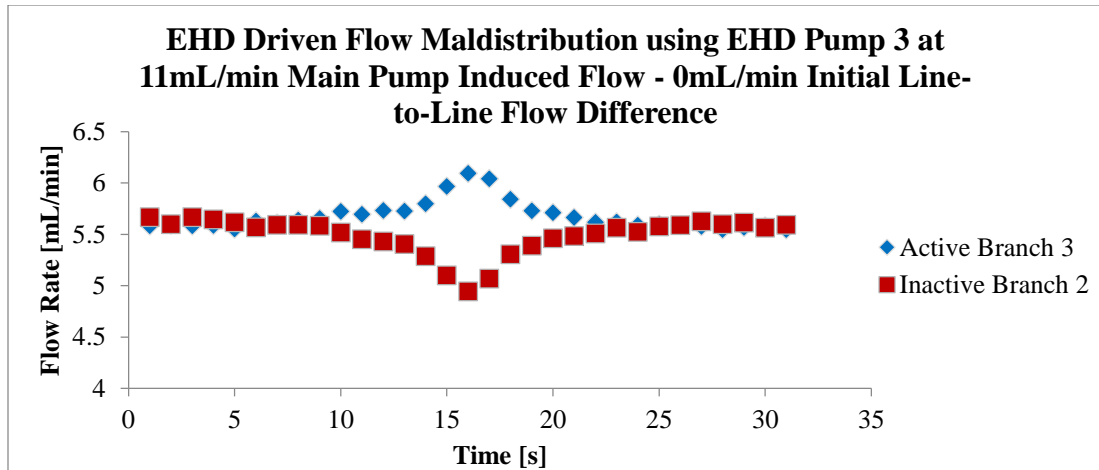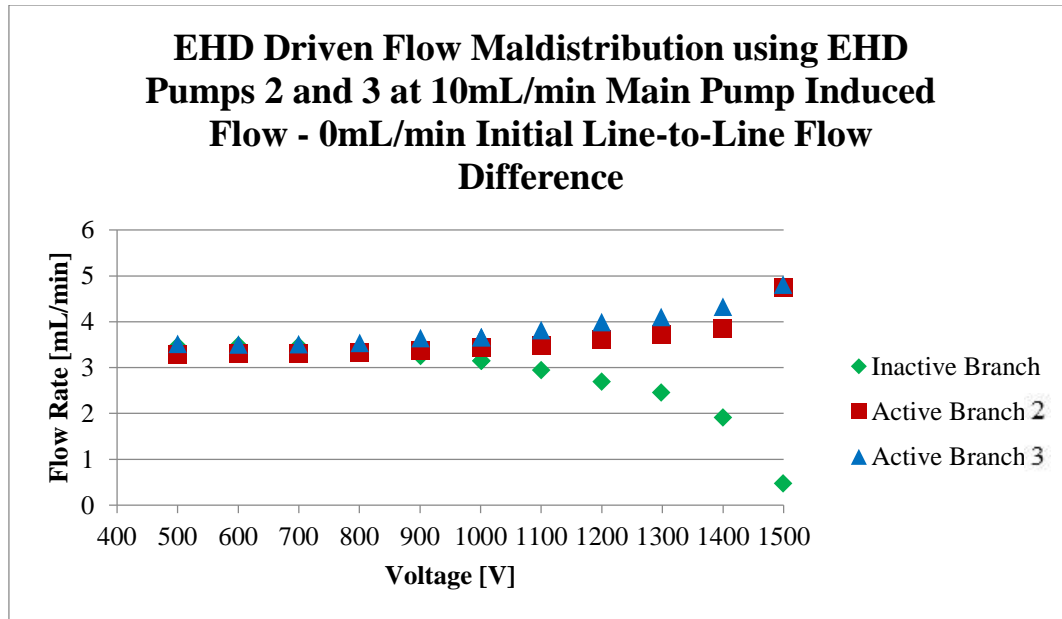


*Figure 24: Flow Maldistribution Characteristics of EHD Pumps 2 and 3 on Channel 1*

The plot shows that at the maximum applied voltage, the EHD Pumps in Channels 2 and 3 are able to create almost completely drain the flow in Channel 1. It can also be seen that at applied voltages of about 0V, the flow rate in all three channels are equal. This is consistent with the desired initial condition of the system. Also noteworthy is the fact that the amount of flow needed in Channels 2 and 3 to decrease the flow in Channel 1 by 3mL/min is about 1.5mL/min per channel, which is consistent with mass conservation.

**Experiment III: Maldistribution to Even Flow Distribution**

### A. Two Branch Experiments

For the first experiment regarding the maldistribution correction capabilities of the EHD system, two channels were utilized; Channel 2 was left open to flow with its associated EHD pump deactivated, Channel 3 was also left open to flow but had its associated EHD pump activated, and Channel 1 was closed to flow entirely. The purpose of this experiment was to investigate the capabilities of the EHD Pump in Channel 3 to generate increased flow in order to equalize the flow in each of the two channels. Due to conservation of mass and considering that the flow going into the distribution manifold is constant, it is implied that increasing the flow in Channel 3 will decrease the flow in Channel 2, demonstrating the desired correction capabilities.

The following plot demonstrated the results obtained when the above configuration is utilized and the applied voltage to EHD Pump 3 is increased in increments of 100V per minute, capping out at 1500V and decreasing back to zero similarly. This was repeated twice to demonstrate continuity and to obtain results that were sufficient for analysis. The flow generated by the main mechanical pump was held constant at 11.5mL/min. Intentional maldistribution of a 1mL flow differential between the channels was introduced through use of a mechanical needle valve.

**Flow Correction using EHD Pump 3 at 11.5mL Main Pump Induced Flow - 1mL/min Line-to-Line Flow Difference**
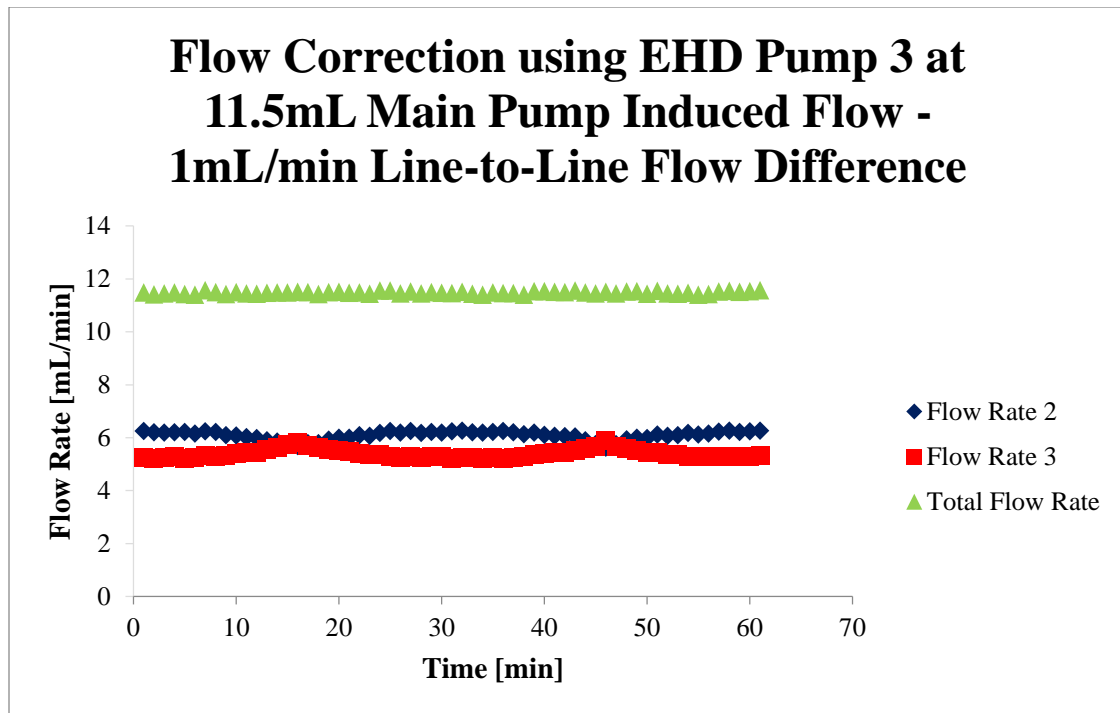
*Figure 25: Maldistribution Correction Characteristic of EHD3 on Channel 2*

On the plot, it is visible that at maximum applied voltages, the EHD pump in Channel 3 is able to not only cause even flow distribution between the two channels, but it is also able to create such a high flow generation that the flow in active Channel 3 surpasses the flow in inactive Channel 2. It can also be seen that at applied voltages of about 0V, there is an interchannel flow differential of about 1mL (as was desired). It is also important to note that the overall flow rate changes very little throughout the experiment.

Figure 18 displays the differential pressures obtained under identical conditions and through similar voltage iterations.
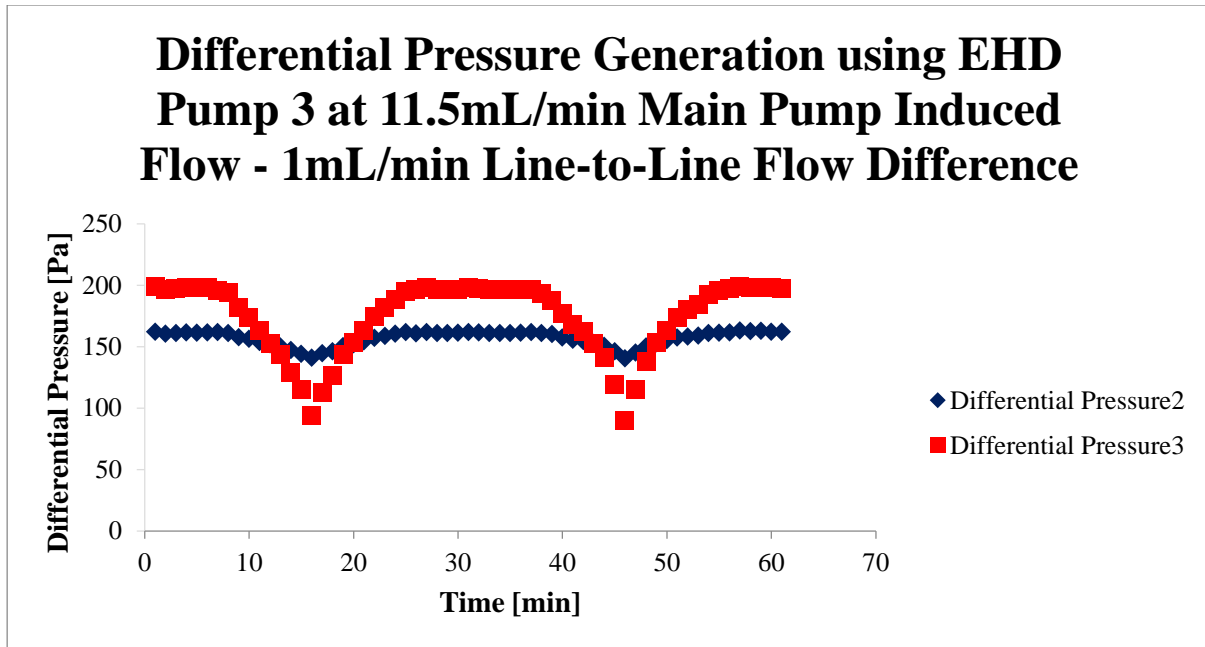
*Figure 26: Differential Pressure Generation of EHD Pump 3 and Corresponding Pressure Increase in Channel 2*

This plot shows that as flow increases in active Channel 3, the differential pressure drops across EHD Pump 3 (consistent with basic fluid mechanics principles and the expected performance of the pump). Similarly, the pressure differential in inactive Channel 2 decreased as flow decreased considering that the EHD Pump in Channel 2 was not activated. It can also be seen that the EHD Pump in Channel 3 was able to produce maximum dynamic pressures of about 100Pa, which is consistent with its performance curves.

For the next experiment, the overall flow rate was increased to a level where the active EHD Pump in Channel 3 was not able to generate pressures high enough for the flow in Channel 3 to surpass the flow in Channel 2. Rather, the maximum applied voltage on the EHD Pump in Channel 3 generated flow that was just sufficient enough to *equalize* the flow between the two channels. This is demonstrated below.
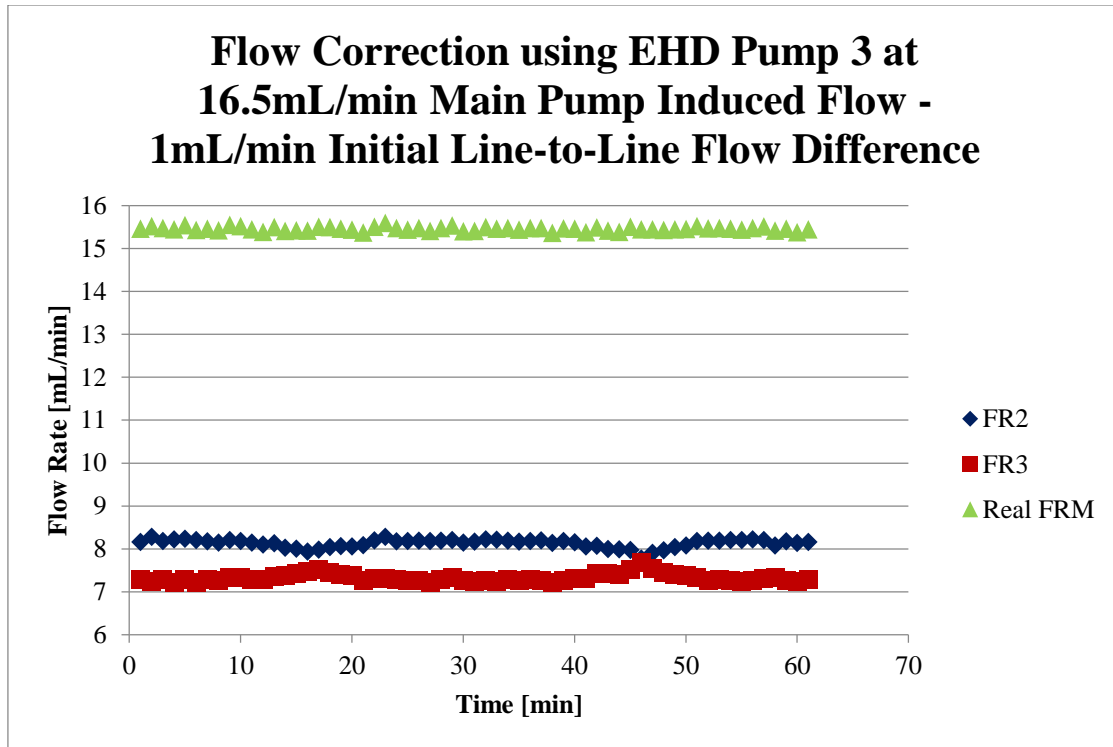
*Figure 27: Maldistribution Correction Capabilities of EHD Pump 3 on Channel 2*

It can be seen that at an applied voltage of 1500V, the flow generation of EHD Pump 3 is just enough to equalize flow in Channel 3. This is because, at higher overall flow rates, the EHD pumps have less influence on the flow in each of the channels. Thus, at a certain "threshold flow rate," EHD Pump 3 is able to produce just enough pressure to equalize the flow rates. This is a very important inherent characteristic of each of the pumps which is crucial in deciding if the EHD pumps are suitable for their particular applications. Similarly, Figure 20 displays the pressure generation characteristics at this overall flow rate. It can also be seen here that the pressures converge, indicating equalized flow between the branch lines.

*Figure 28: Differential Pressure Generation Characteristic of EHD Pump 3 and Corresponding Pressure Change in Channel 2*

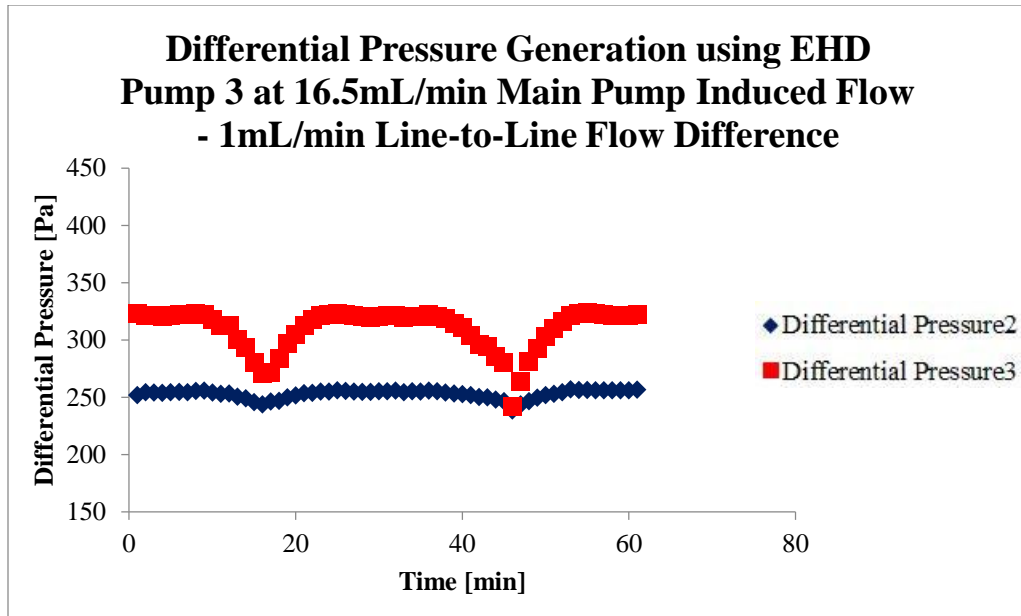Additional graphs can be seen in the Appendix of this report indicating that at induced overall flow rates of more than 16.5mL/min, active EHD Pump 3 is incapable of producing pressures that generate flow that is significant enough to cause the flows in the two branch lines to converge. This is because pressure generation at high flow rates has a less significant effect on the interchannel system while still affecting the active channel. This is also a repeatable phenomenon as indicated by the multiple experimental iterations in the graph.

## B. Three Branch Experiment

For this experiment regarding the maldistribution correction capabilities of the EHD system, all three channels were utilized; both Channel 2 and Channel 3 EHD pumps were active, while Channel 1 EHD pump was left inactive. All three branches remained open at all times. The purpose of this experiment was to investigate the capabilities of the EHD pumps in active Channels 2 and 3 to generate increased flow in order to equalize the flow in all channels. Due to

conservation of mass and considering that the flow going into the distribution manifold is constant, it is implied that increasing the flow in Channels 2 and 3 will decrease the flow in Channel 1, demonstrating the desired correction capabilities.

The following plot demonstrates the results obtained when the above configuration was utilized and the applied voltages to EHD Pumps 2 and 3 are increased simultaneously in increments of 100V per minute, capping out at 1500V. This was repeated twice to reassure continuity and to obtain results that were sufficient for analysis. The flow generated by the main mechanical pump was held constant at 17.3mL/min. Intentional maldistribution of a 1.75mL flow differential between Channel 1 and Channels 2 and 3 was introduced through use of a mechanical needle valve.
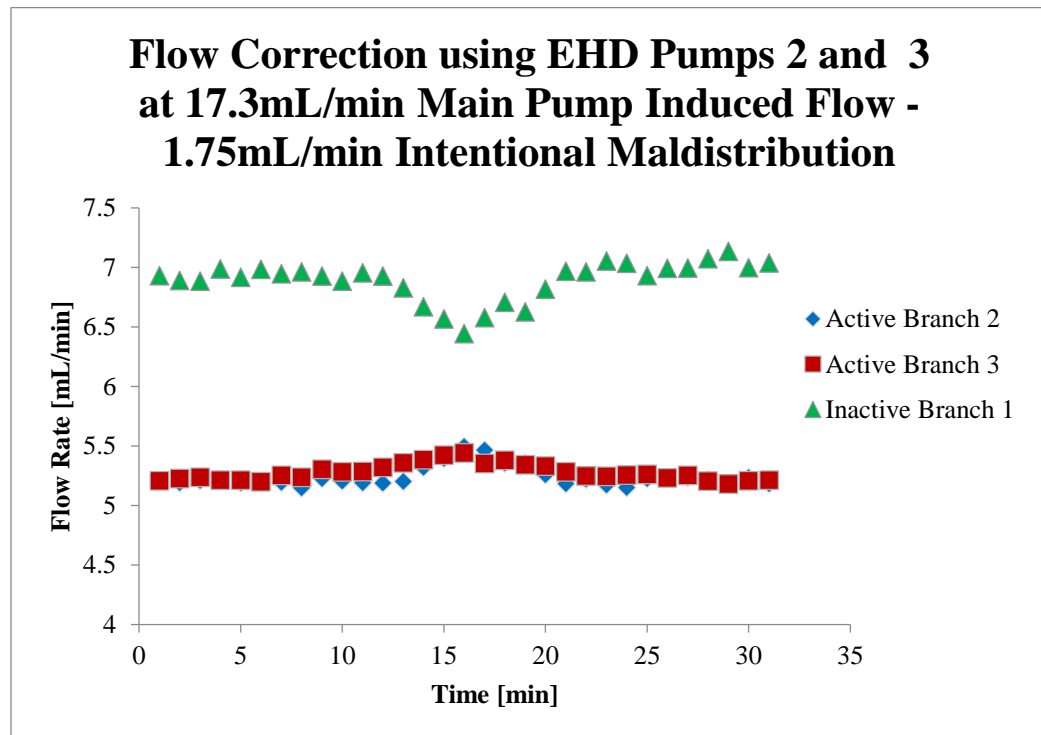


Figure 29: Maldistribution Correction Capabilities of EHD Pumps 2 and 3 on Channel 1

On the plot, it is visible that at maximum applied voltages, the EHD Pumps in Channels 2 and 3 are not able to cause even flow distribution due to the high initial flow rate difference between active Channels 2 and 3 and inactive Channel 1. Despite the fact that flow rates do not even out, the EHD pumps 2 and 3 have a significant effect on the flow rate of Channel 1. At 1500V, the difference between the flow rates was 1mL/min. Flow rates would converge if EHD Pumps 2 and 3 are subjected to a higher voltage, yet this was not tested due to safety reasons related to the rated voltages of these particular EHD pumps. It is also important to note that the overall flow rate changes insignificantly throughout the experiment.

The next plot presents the pressure differences across each EHD pump. Plotting each pressure difference as a function of time yields that active EHD Pumps 2 and 3 generate higher pressure drops compared to inactive EHD Pump 1 when subjected to high voltage.
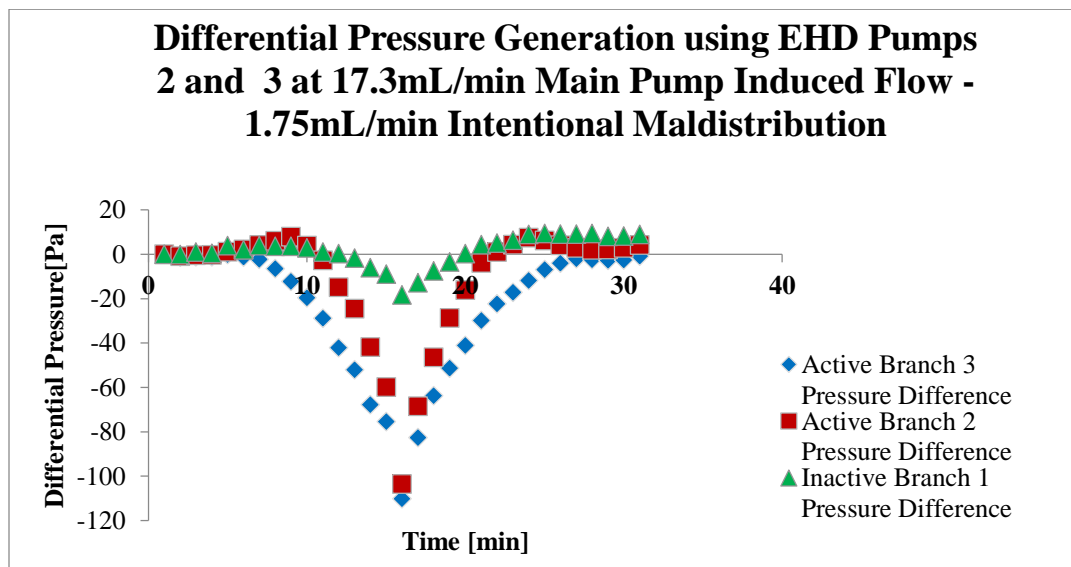


*Figure 30: Pressure Generation Capabilities of EHD Pumps 2 and 3 on inactive EHD Pump 2*

In conclusion, the EHD conduction pumping phenomenon is present and functions effectively in meso-scale pumping.

**Conclusion**

The research value presented in this Major Qualifying Project is its investigation of an advanced and innovative system of fluid flow generation and distribution control and its application in a meso-scale single-phase flow experimental setup. This study resulted in observing the EHD conduction pumping phenomenon successfully controlling the fluid flow along three parallel branches. The size of the assembled loop was far greater than the size of the EHD conduction pumps; nonetheless, an EHD pump active branch was able to effectively reduce the flow rate in an inactive branch on demand. The setup allowed for easy flow maldistribution correction by varying the voltage applied to the EHD conduction pumps.

Fluid flow was successfully generated and flow distribution control was achieved using EHD conduction pumps in parallel branches. It was shown that flow rates and pressure drops across the parallel branches were sufficient to affect the flow distribution between the branches. In conclusion, EHD conduction driven flow distribution is a successful technology in the meso-scale domain, capable of functioning in a multi-branch setup. Applications in extraterrestrial environments, large industrial thermal systems, and even microelectronics that require enhancement in heat transfer could take advantage of an EHD conduction driven fluid circulation system. EHD conduction pumping is a promising alternative solution to modern day flow distribution control systems using traditional technologies.

# References

[1] J. Seyed-Yagoobi, 2005, "Electrohydrodynamic pumping of dielectric liquids", Journal of Electrostatics, vol. 63, pp. 861-869.

[2] P. Atten, J. Seyed-Yagoobi, 2003, "Electrohydrodynamically Induced Dielectric Liquid Flow Through Pure Conduction in Point/Plane Geometry", IEEE Transactions on Dielectrics and Electrical Insulation, vol. 10, pp. 27-36.

[3] V. K. Patel, J. Seyed-Yagoobi, 2011, "Dielectric fluid flow generation in meso-tubes with micro-scale electrohydrodynamic conduction pumping", Proceedings of the IEEE International Conference on Dielectric Liquids, pp. 1–4.

[4] M. R. Pearson and J. Seyed-Yagoobi, "Experimental study of EHD conduction pumping at the meso- and micro-scale", Journal of Electrostatics, vol. 69, pp. 479-485.

[5] M. R. Pearson, J. Seyed-Yagoobi, 2009, "Advances in Electrohydrodynamic Conduction Pumping", IEEE Transactions on Dielectrics and Electrical Insulation, vol. 16, pp. 424-434.

[6] Y. Feng, J. Seyed-Yagoobi, 2004, "Control of Liquid Flow Distribution Utilizing EHD Conduction Pumping Mechanism", Conference Record of the 39th IEEE IAS Annual Meeting, vol. 4, pp. 2345-2352.

[7] V. K. Patel, F. Robinson, J. Seyed-Yagoobi, 2013, "Terrestrial and Microgravity Experimental Study of Microscale Heat-Transport Device Driven by Electrohydrodynamic Conduction Pumping", IEEE Transactions on Industry Applications, vol. 49, pp. 2397-2401.

**Appendices**

**Appendix A: Novec 7600 Engineering Fluid Physical Properties**

## Typical Physical Properties

| | Properties | 3M™ Novec™ 7600 Engineered Fluid |
|---|---|---|
| Not for specification purposes. All values @ 25°C unless otherwise specified. | Boiling Point (°C) | 131 |
| | Pour Point (°C) | -98 |
| | Molecular Weight | 346 |
| | Boiling Point (°C) @ 760 mmHg | 98.0 |
| | Freeze Point (°C) | -38 |
| | Liquid Density (g/ml) | 1540 kg/m³ |
| | Coefficient of Expansion | 0.00114 K⁻¹ |
| | Latent Heat of Vaporization @ 1 atm. (kJ/kg) | 115.6 |
| | Surface Tension (dynes/cm) | 17.7 |
| | Kinematic Viscosity (cSt) | 1.07 |
| | Critical Temperature (°C) | 260 |
| | Critical Pressure (Mpa) | 1.67 |
| | Solubility of Solvent in Water (ppb) | <10 ppm by weight |
| | Solubility of Water in Solvent (ppb) | 410 ppm by weight |
| | Dielectric Strength, 2.54 mm gap (kV) | 31 |
| | Volume Resistivity | $3 \times 10^{10}$ ohm-cm |
| | Dielectric Constant | 6.4 |

**Appendix B-1: Solidworks Drawing of EHD Pumps Support Design**
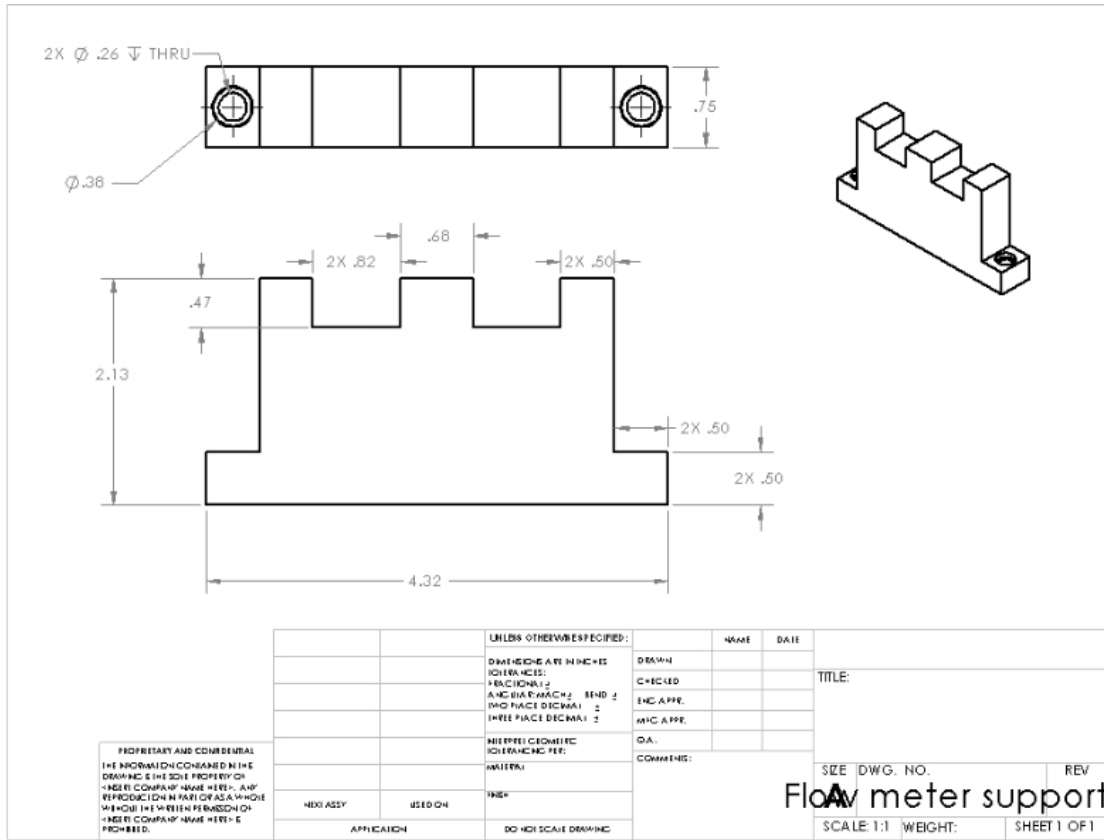
**Appendix B-2: Solidworks Drawing of Flow Meter Support Design**
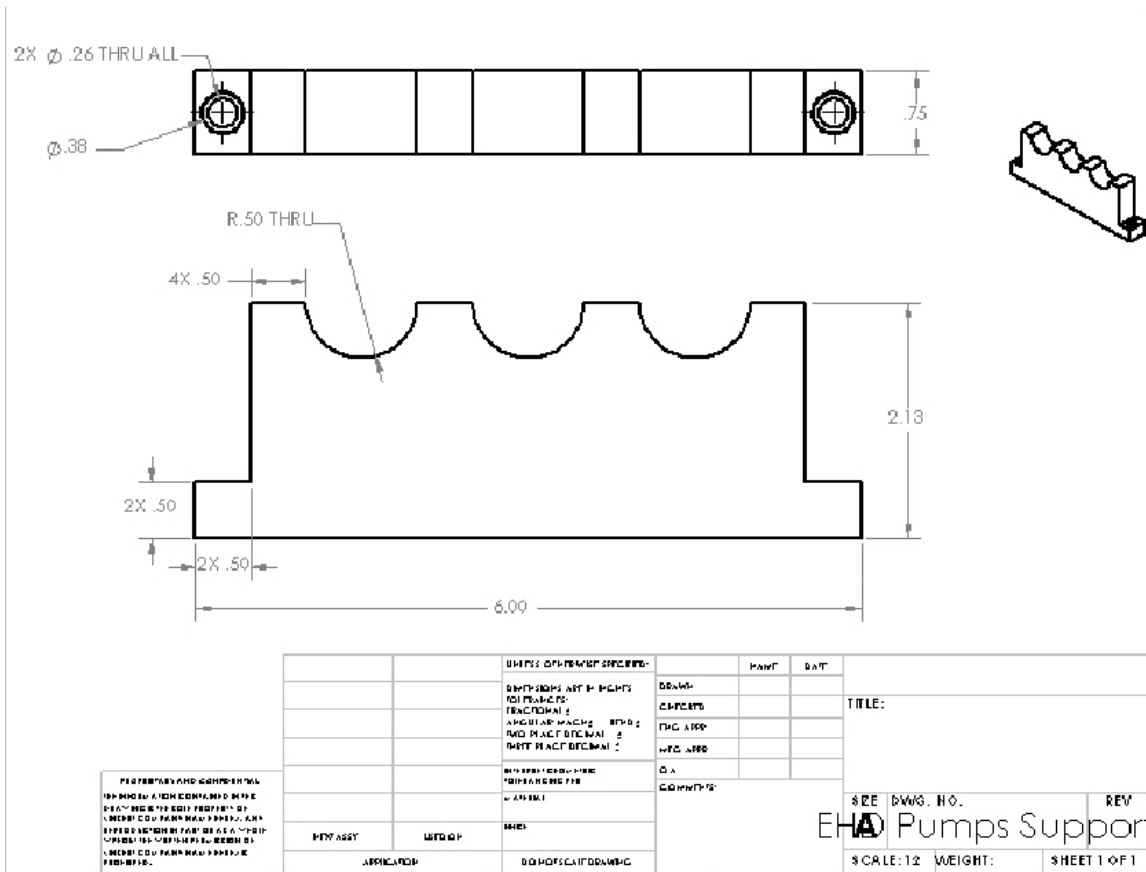
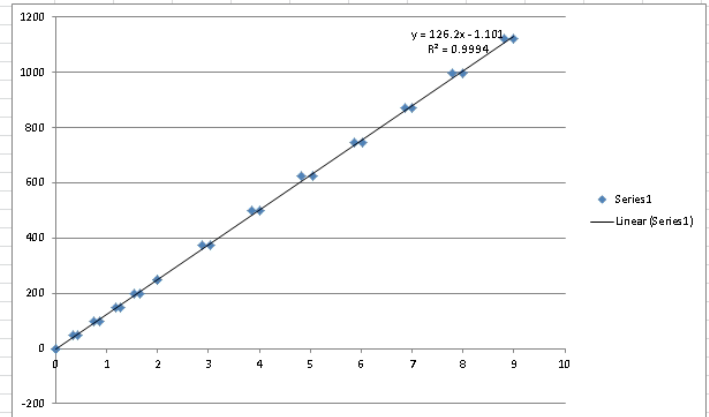## Appendix C-1: Calibration Data and Calibration Curves for Pressure Transducer 1

| Name EHD-DP1 | | | Voltage | Pascal | Inches of water column |
|---|---|---|---|---|---|
| Date | | Dash #22 | 1.9 | 0 | 0 |
| 2/5/2015 | | | 8.93 | 1121.28 | 4.5 |
| | | | 8.18 | 996.696 | 4 |
| By : | | | 7.38 | 872.109 | 3.5 |
| CJ,KM,BS | | | 6.58 | 747.522 | 3 |
| | | | 5.77 | 622.935 | 2.5 |
| | | | 4.99 | 498.348 | 2 |
| | | | 4.24 | 373.761 | 1.5 |
| | | | 3.39 | 249.174 | 1 |
| | | | 3.05 | 199.339 | 0.8 |
| | | | 2.74 | 149.504 | 0.6 |
| | | | 2.35 | 99.6696 | 0.4 |
| | | | 2.1 | 49.8348 | 0.2 |
| | | | 1.9 | 0 | 0 |
| 2.34 | 49.8348 | | | | 0.2 |
| 2.64 | 99.6696 | | | | 0.4 |
| | | | 2.94 | 149.504 | 0.6 |
| | | | 3.26 | 199.339 | 0.8 |
| | | | 3.45 | 249.174 | 1 |
| | | | 4.22 | 373.761 | 1.5 |
| | | | 4.93 | 498.348 | 2 |
| 5.94 | 622.935 | | | | 2.5 |
| | | | 6.54 | 747.522 | 3 |
| | | | 7.33 | 872.109 | 3.5 |
| | | | 8.12 | 996.696 | 4 |
| | | | 8.93 | 1121.28 | 4.5 |

$$y = 158.53x - 293.95$$
$$R^2 = 0.9993$$



## Appendix C-2: Calibration Data and Calibration Curves for Pressure Transducer 2

| Name EHD-DP2 | | | Voltage | Pascal | Inches of water column |
|---|---|---|---|---|---|
| Date | | Dash #22 | 0.01 | 0 | 0 |
| 2/6/2015 | | | 9.18 | 1121.28 | 4.5 |
| | | | 8.32 | 996.696 | 4 |
| By : | | | 7.32 | 872.109 | 3.5 |
| CJ,KM,BS | | | 6.28 | 747.522 | 3 |
| | | | 5.2 | 622.935 | 2.5 |
| | | | 4.22 | 498.348 | 2 |
| | | | 3.15 | 373.761 | 1.5 |
| | | | 2.06 | 249.174 | 1 |
| | | | 1.65 | 199.339 | 0.8 |
| | | | 1.25 | 149.504 | 0.6 |
| | | | 0.77 | 99.6696 | 0.4 |
| | | | 0.33 | 49.8348 | 0.2 |
| | | | 0.02 | 0 | 0 |
| | | | 0.66 | 49.8348 | 0.2 |
| | | | 0.95 | 99.6696 | 0.4 |
| | | | 1.35 | 149.504 | 0.6 |
| | | | 1.77 | 199.339 | 0.8 |
| | | | 2.15 | 249.174 | 1 |
| 2.93 | 373.761 | | | | 1.5 |
| 3.95 | 498.348 | | | | 2 |
| 4.94 | 622.935 | | | | 2.5 |
| | | | 6.16 | 747.522 | 3 |
| | | | 7.08 | 872.109 | 3.5 |
| | | | 8.07 | 996.696 | 4 |
| | | | 9.18 | 1121.28 | 4.5 |

$$y = 122.34x - 8.4335$$
$$R^2 = 0.9992$$
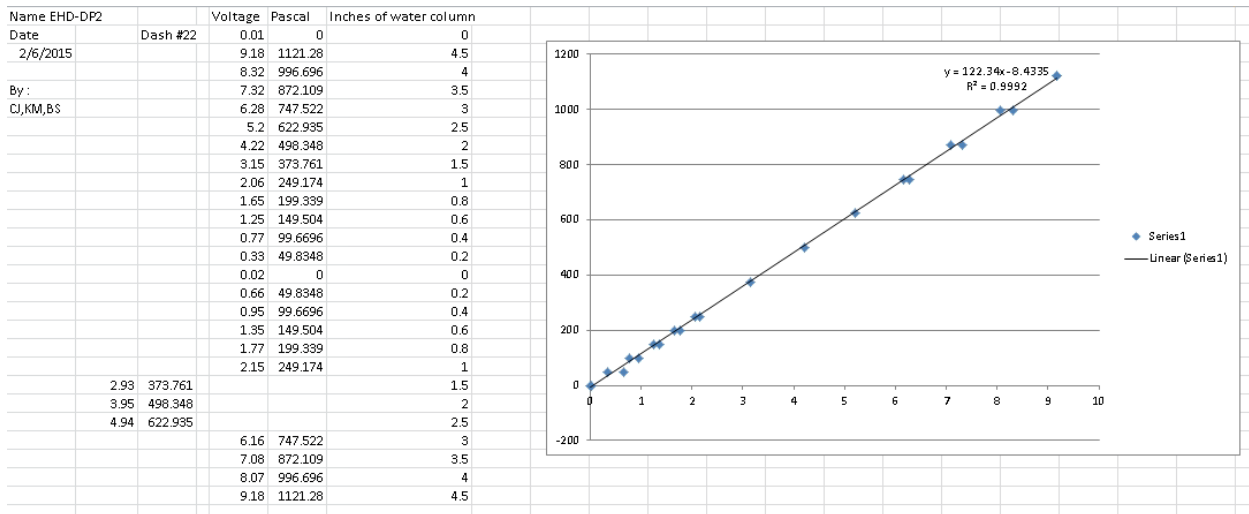
## Appendix C-3: Calibration Data and Calibration Curves for Pressure Transducer 3

| Name EHD-DP3 | | Voltage | Pascal | Inches of water column |
|---|---|---|---|---|
| Date | Dash #24 | 0 | 0 | 0 |
| 2/5/2015 | | 8.98 | 1121.28 | 4.5 |
| | | 8 | 996.696 | 4 |
| By : | | 7 | 872.109 | 3.5 |
| CJ,KM,BS | | 6.03 | 747.522 | 3 |
| | | 5.04 | 622.935 | 2.5 |
| | | 4 | 498.348 | 2 |
| | | 3.04 | 373.761 | 1.5 |
| | | 2 | 249.174 | 1 |
| | | 1.54 | 199.339 | 0.8 |
| | | 1.18 | 149.504 | 0.6 |
| | | 0.74 | 99.6696 | 0.4 |
| | | 0.35 | 49.8348 | 0.2 |
| | | 0 | 0 | 0 |
| | | 0.43 | 49.8348 | 0.2 |
| | | 0.87 | 99.6696 | 0.4 |
| | | 1.28 | 149.504 | 0.6 |
| | | 1.65 | 199.339 | 0.8 |
| | | 2 | 249.174 | 1 |
| | | 2.87 | 373.761 | 1.5 |
| | | 3.85 | 498.348 | 2 |
| | | 4.83 | 622.935 | 2.5 |
| | | 5.86 | 747.522 | 3 |
| | | 6.86 | 872.109 | 3.5 |
| | | 7.8 | 996.696 | 4 |
| | | 8.8 | 1121.28 | 4.5 |



$y = 126.2x - 1.101$
$R^2 = 0.9994$

## Appendix D: Calibration Data and Calibration Curves for Main Flow Meter

| Name FR Main | Voltage | Flow Rate Displayed | Actual Flow Rate |
|---|---|---|---|
| Date | 0.29232 | 1.6 | 6 |
| 2/5/2015 | 0.3323 | 2.35 | 6.8 |
| | 0.35729 | 3.3 | 7.3 |
| By : | 0.38477 | 4.48 | 7.85 |
| CJ,KM,BS | 0.42225 | 5.33 | 8.6 |
| | 0.47222 | | 9.6 |
| | 0.55966 | 9.9 | 11.35 |
| | 0.62213 | 12.95 | 12.6 |
| | 0.67959 | 16.1 | 13.75 |
| | 0.75205 | 19.3 | 15.2 |
| | 0.81201 | 23.7 | 16.4 |



$y = 39.588x^2 - 2.0497x - 1.0527$
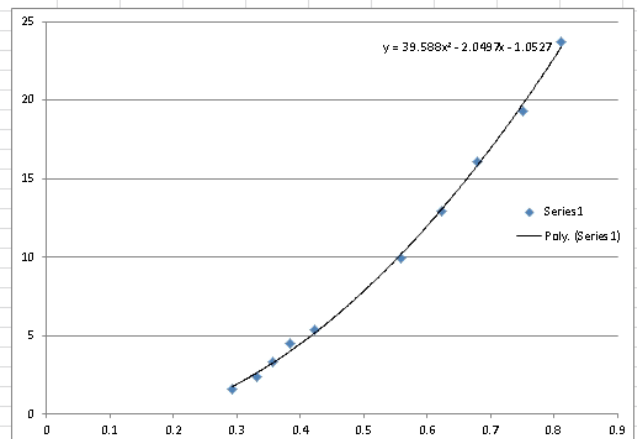
**Appendix E-1: LabVIEW Block Diagram (Overview)**
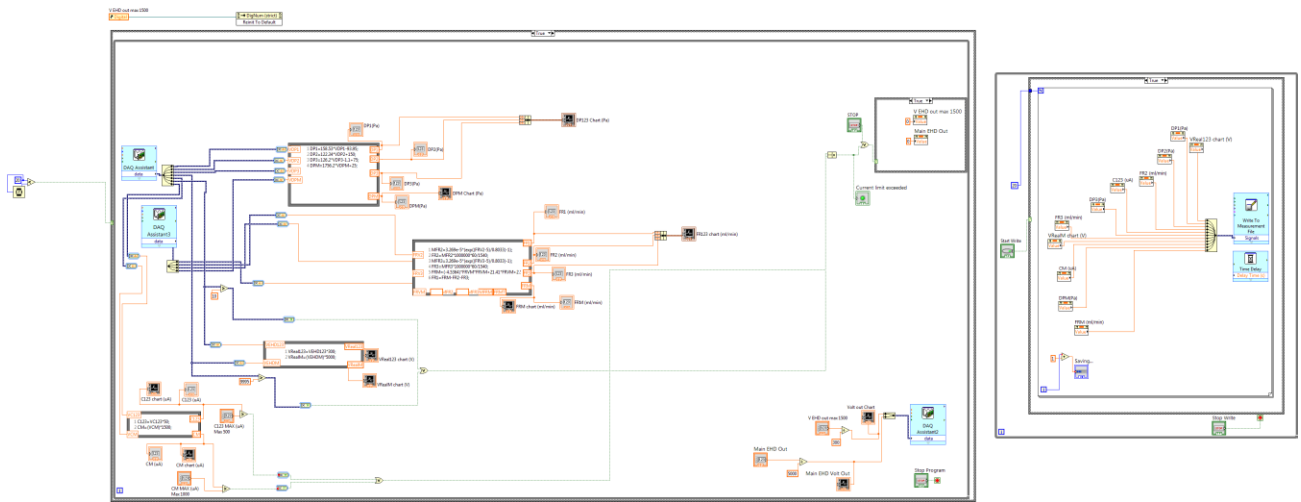


**Appendix E-2: LabVIEW Block Diagram (Section I)**
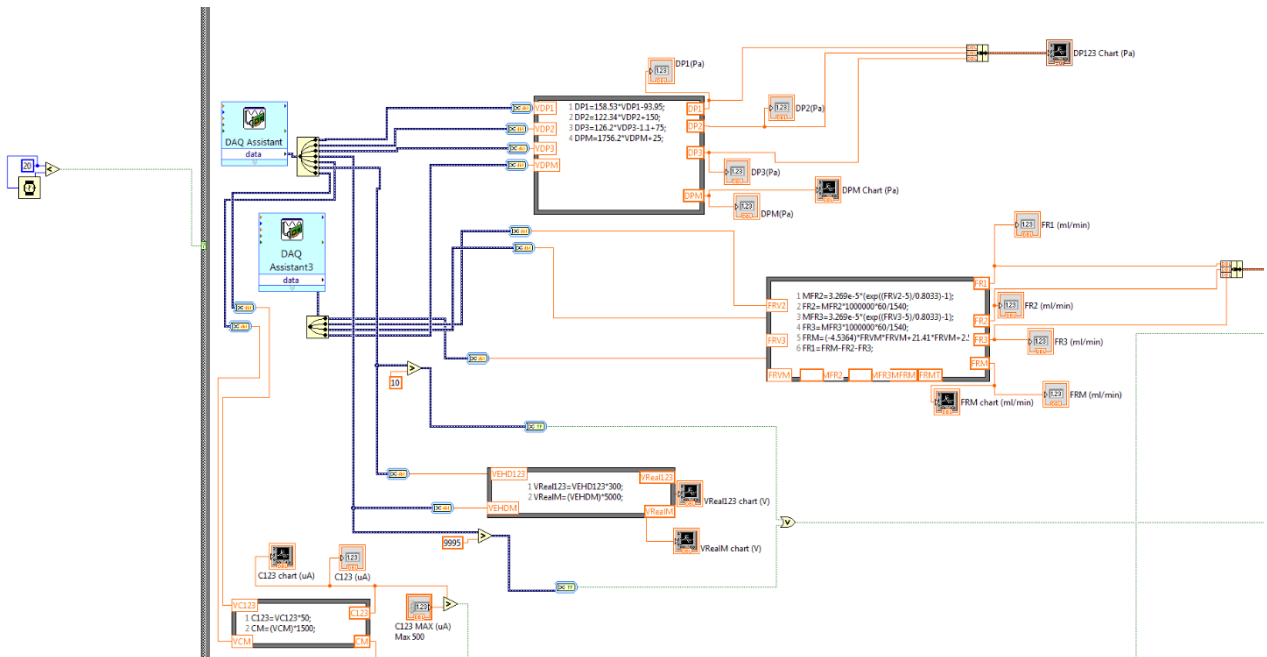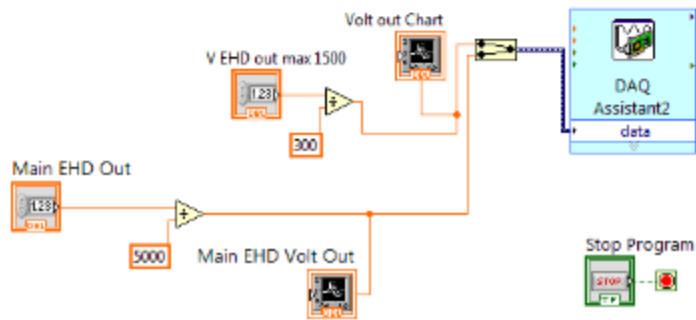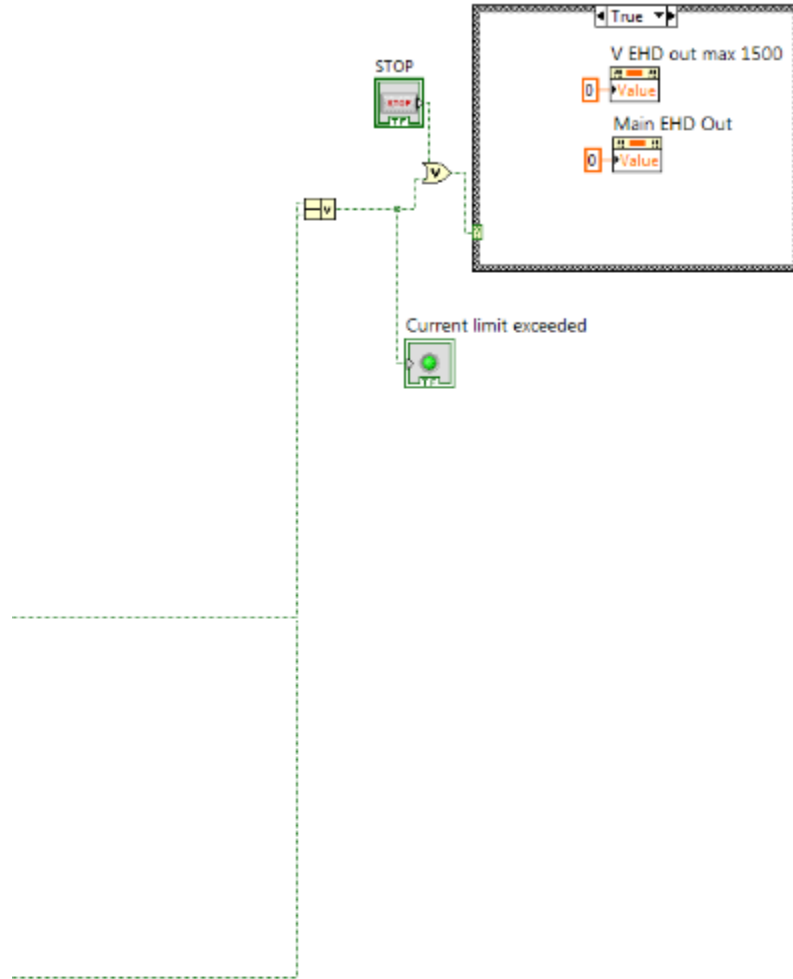
**Appendix E-3: LabVIEW Block Diagram (Section II)**
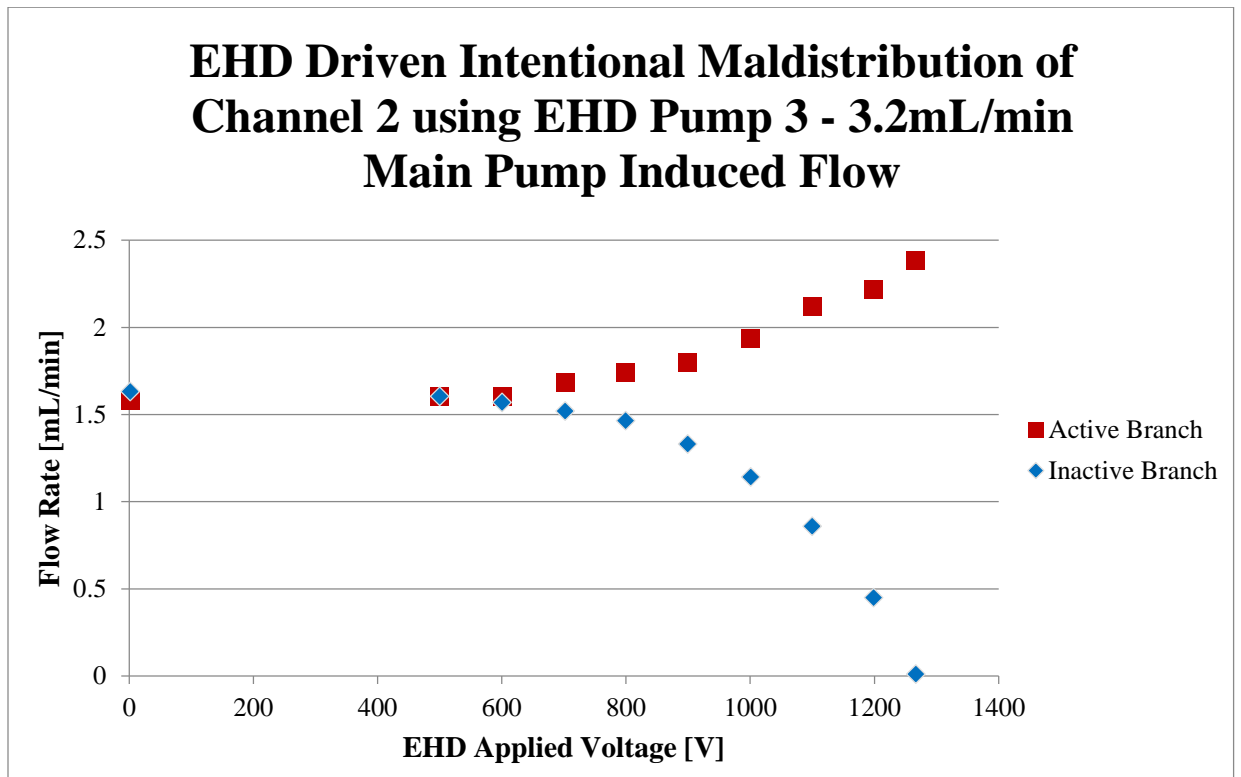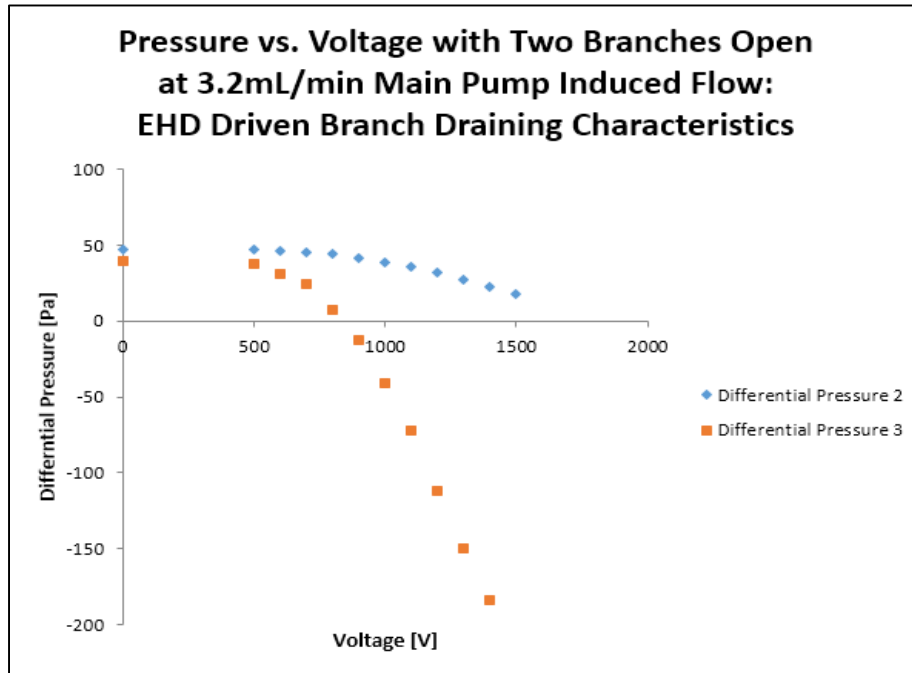
**Appendix E-3: LabVIEW Block Diagram (Section III)**
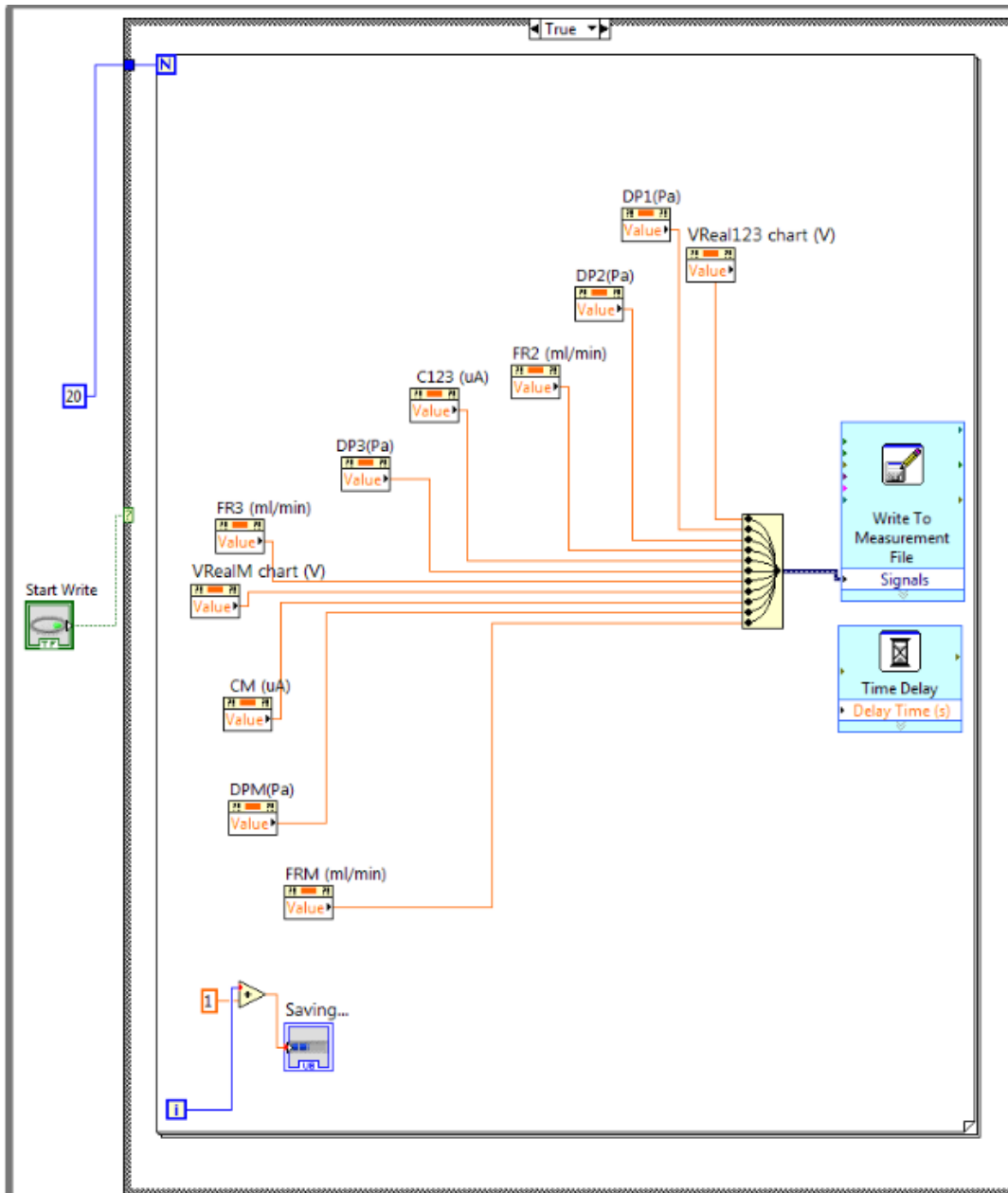
**Appendix F-1: EHD Driven Intentional Maldistribution of Channel 2 using EHD Pump 3**



EHD Driven Intentional Maldistribution of Channel 2 using EHD Pump 3 - 3.2mL/min Main Pump Induced Flow

**Appendix F-2: Two-Channel Pressure Generation and Effects**



**Appendix F-3: Three-Channel Pressure Generation and System Effects**